DIMENSIONAL STABILITY OF UHMW-PE PARTS: INFLUENCE OF AGING AND CROSSLINKING

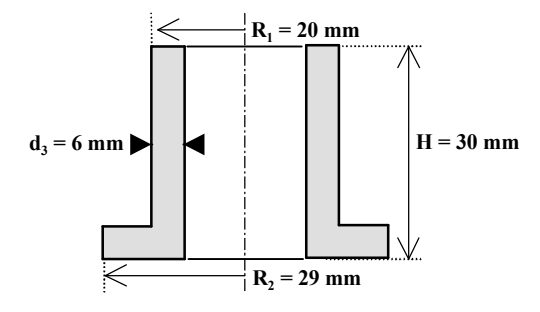
Y.Dirix, A. Becker, M. Wiederkehr, H. Schmotzer, R. Lerf.

PI Precision Implants AG,. Schachenallee 29, 5001 Aarau, Switzerland Switzerland

INTRODUCTION: Ultra high molecular weight polyethylene is the main material used as a bearing surface in total hip or knee replacements due to it's high toughness and wear resistance. However, as a result of the extremely high (> 10⁶ gr/mol) molecular weight and thus high melt viscosity, UHMW-PE powders cannot be processed using screw extruders. Instead, sheet compression molding or ram extrusion techniques are used to sinter the particles into a preform. This preform is machined into the desired implant, packaged, sterilized and after a shelflife period implanted. Additionally, highly crosslinked polyethylenes have been developed by irradiating (γ or e-beam) the preforms in the solid or molten state, followed by a thermal treatment to enhance the cross-linking process. The long term dimensional stability of polyethylene part is important for the bearing surface and, due to the modularity of many hip and knee systems, also for the connectors which snap into a metal backing. Here, the influence of the processing steps on the dimensional stability of machined UHMW-PE parts is investigated. The dimensional changes during shelflife or clinical use are mimicked using accelerated aging tests which corresponds with 5-10 yr. Shelflife¹ or 4yr. clinical use²

METHODS: Sheet compression molded material (GUR 1020) was purchased at PolyHiSolidur, Vreden Germany. Test specimens as shown in Fig 1, were produced from untreated and crosslinked UHMW-PE and tested according to the matrix shown in Table 1.

Figure 1: Cross section of test cylinders



<u>Crosslinking</u>: The UHMW-PE was preheated at 125°C, irradiated with e-beam (7 Mrad) and

subsequently remelted before it was slowly cooled down

<u>Sterilization</u>: The samples were packaged under nitrogen atmosphere and sterilized using 3 Mrad γ radiation.

Aging was done according to ASTM F2003-00, method B. The cylinders were inserted for 14 days in a vessel at 5 atm. oxygen pressure and 70°C.

The <u>Dimensions</u> of the cylinders were measured on the inside and outside at a height of 12, 18 and 24 mm using a 3-D coordinate measuring machine (Mitutoyo Euro C9106, accuracy 3 μ m). Samples were thermostated at $20 \pm 1.0^{\circ}$ C. The roundness is defined as the difference between the maximum and minimum radius³. Data presented here are averaged over at least 8 cylinders. Cross comparison of the data was done using the T-test (sigmastat software).

Table 1: Test matrix for cylindrical specimens

X-linked	Sterilized	Aged	Code
No	No	No	Gur
No	No	Oxygen	Gur Aged-O ₂
No	Yes	No	Gur St
No	Yes	Oxygen	Gur St +Aged O ₂
No	Yes	Nitrogen	Gur St +Aged N ₂
Yes	No	No	X-linked
Yes	No	Oxygen	X-linked+Aged O ₂

RESULTS: During aging, all cylinders slightly deformed into an ellipsoid as could be observed on all height levels. As an example, the dimensions of crosslinked polyethylene before and after aging in oxygen are shown in Figure 2. (pls. note the scale!). The roundness values are shown in Figure 3. The highest deviation from roundness is observed for the sterilized and oxygen aged material (Gur St+Aged O₂). There is no statistical difference between the UHMW-PE as-machined (GUR), the aged PE (GUR Aged O₂), the sterilized PE (GUR St) and the sterilized PE aged in nitrogen (Gur St+Aged N2). However there is a statistical difference (P<0.05) between the sterilized and oxygen aged UHMW-PE (Gur St+Aged O₂) and all the other materials. Finally, aging of crosslinked PE results in a significant (P<0.001) increase in roundness.

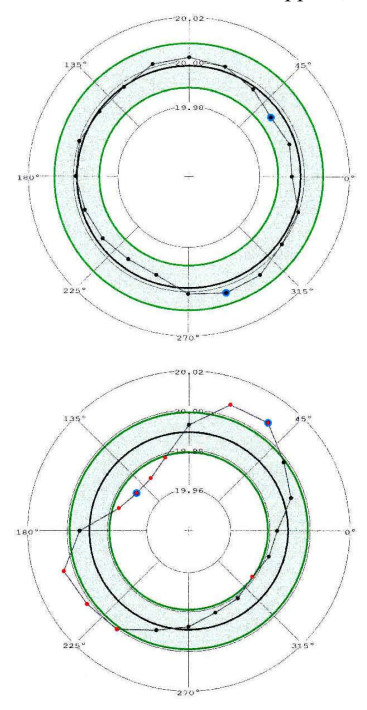


Figure 2: Top view of outer dimensions at 24 mm height for X-linked UHMW-PE as machined (top) and after aging in oxygen (bottom).

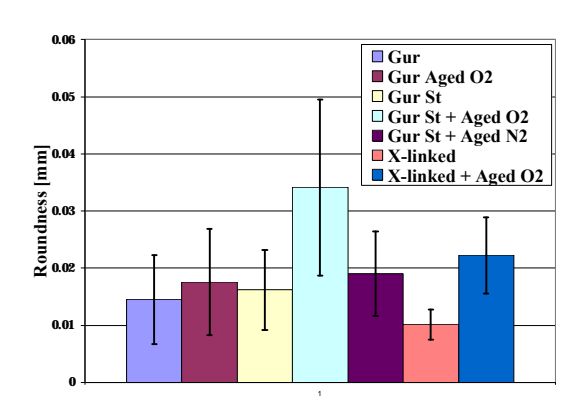


Figure 3: Roundness for the test cylinders, outer diameter at H = 24 mm.

DISCUSSION & CONCLUSIONS: During the sheet molding process, the UHMW-PE is subjected to thermal/mechanical cycles which influences the density, homogeneity and amount of residual stresses in the material, which are also present in the cylinders. Release of these stresses results in a small deformation into an ellipsoid (Figure 2). The highest deviation from a perfect cylinder is observed for the UHMW-PE that has been sterilized and aged in oxygen at 70° C. There is no difference between the as-machined (GUR), the aged (Gur Aged O₂) and the sterilized part (Gur St), i.e., the combination of γ-sterilization and thermal activation in an oxygen environment causes the dimensional change. During the γ-sterilization,

chain scission in PE occurs resulting not only in a small amount of crosslinks, but also free radicals that are trapped into the material⁴. These radicals are reactive towards oxygen at elevated temperature leading to a cascade of oxidative reactions⁵. Consequently the molecular weight decreases enabling a release of the internal stresses. These degradative reactions can not occur in an inert nitrogen atmosphere (Gur St+Aged N2). For the production of the highly cross-linked polyethylene, a large amount of chain scission and free radicals has been generated on purpose. Afterwards the preform is remelted and slowly cooled down. Consequently, the free radicals are eliminated and the residual stresses are reduced. Therefore, the dimensional change after aging in oxygen is lower compared to the sterilized and aged Gur materials. To summarize, accelerated aging in oxygen of sterilized UHMW-PE leads to a dimensional change twice the deviation from roundness after machining.

REFERENCES:

¹Sanford W.M. et al., Trans. ORS 42, 21:23, 1996, ²Mc Kellop H. et al., Trans ORS 42, 21: 483, 1996, ³VSM 10204, Normen Auszug, 9th ed., 1986, ⁴ Kurtz S.M., et al., Biomaterials 20, 1659, 1999 ⁵ Premnath V., et al., Biomaterials 17, 1741, 1996

NEW HYDRAULIC CEMENTS BASED ON a-TRICALCIUM PHOSPHATE - CALCIUM SULFATE DIHYDRATE MIXTURES

M. Bohner, H. Schmid

Dr hc Robert Mathys Foundation, Bischmattstrasse 12, CH-2544 Bettlach, Switzerland

INTRODUCTION: Calcium phosphate cements based on a-tricalcium phosphate (a-TCP) - water mixtures have been studied extensively for the last 20 years. Despite these efforts, there is still a need for new alternatives to increase their injectability and create macropores. Here, we propose to study the effect of calcium sulfate dihydrate (CSD) on a-TCP - water mixtures. Several series of experiments were performed where the following factors were varied: (i) the CSD fraction; (ii) the di-sodium hydrogen phosphate dihydrate (DSHPD) concentration in the mixing liquid; and (iii) the amount of mixing liquid.

MATERIALS AND METHODS: The cement samples contained 4.0g powder (a-TCP + CSD) and 1.72mL solution. The CSD amount was varied from 0 to 1.11g, whereas the DSHPD concentration in the mixing solution was in the range of 0.05 to 0.40M. The cement ingredients were mixed for 45s with a spatula in a small beaker. The paste was then placed into two syringes whose end had been previously cut off. The setting time was measured using a so-called penetrometer. Fifteen minutes after setting, the samples were placed into 10mL of 0.15M phosphate buffer solution at 37°C. After one or two days of incubation, the samples were taken out and dried in air at 37°C and later at 110°C until a constant weight was reached. The sides of the cylindrical samples were then flattened, and characterized by measuring the apparent density, the diametral tensile strength, the crystalline composition via x-ray diffraction (XRD), and the specific surface area (BET). Solubility calculations were performed using known solubility data.

RESULTS: A twofold decrease of the cement setting time was observed when 0.1-0.2g of CSD were added into the cement. This sharp decrease was followed by a slow increase of the setting time. Interestingly, the position of the setting time minimum increased towards larger CSD amounts when the phosphate concentration of the mixing solution was increased. Furthermore, the minimum became lower, much broader and flatter. These results suggest an interaction between the CSD

amount and the phosphate concentration. An increase of the phosphate concentration in the mixing liquid led to a decrease of the setting time. A decrease of setting time was also observed when the amount of mixing liquid was decreased. The apparent density of the cement decreased with an increase of the CSD amount, whereas the diametral tensile strength of the cement was rather independent of the CSD amount, the incubation time, or the DSHPD concentration. The specific surface area of the cement samples was increased by the addition of 0.1-0.2g of CSD. However, hardly any changes were observed beyond 0.2g CSD. An increase of the phosphate concentration from 0.1 to 0.2M provoked a small but significant decrease of the specific surface area, but only after one day of incubation. Interestingly, an increase of the incubation time led to a small decrease of the specific surface area. The XRD spectra show that the cement samples contained a mixture of apatite, CSH (resulting from heating up CSD at 110°C) and a-TCP. The peak intensities indicated that the relative intensity of the CSH peak was null below 0.2g CSD and then steadily increased. Simultaneously, the a-TCP peak rapidly increased with a small increase of the CSD amount and then remained stable or even slightly decreased. Interestingly, the phosphate concentration had no effect on the CSH relative peak intensity, but had a large effect on that of a-TCP: a larger phosphate concentration led to larger a-TCP peaks. The results were similar at two days apart from a decrease of the size of the a-TCP peaks.

DISCUSSION: Based on solubility calculations, the present setting time results can be explained according to 4 different effects: (i) CSD increases the supersaturation towards HA/CDHA in the mixing liquid, hence resulting in a decrease of setting time (for small CSD amount); (ii) The dissolution of CSD decreases the solubility of a-TCP in the mixing liquid, hence leading to a slower setting reaction (for large CSD amount); (iii) The presence of phosphate ions in the mixing solution increases the supersaturation towards HA/CDHA in the mixing liquid, hence leading to a shortening of the setting time (for large phosphate concentrations); (iv) The phosphate ions of the mixing liquid react with calcium ions stemming from CSD dissolution, hence increasing the saturation

European Cells and Materials Vol. 5. Suppl. 1, 2003 (pages 3-4) of the mixing solution toward CSD, and decreasing the dissolution rate of CSD (valid at large CSD amount).

CONCLUSION: CSD can be used in combination with phosphate ions to control the setting time of a-TCP - water mixtures, without affecting their mechanical properties.

COMPLEMENTARY TECHNIQUES IN THE EVALUATION OF ELECTROCHEMICAL DEGRADATION OF SOME IMPLANT METALLIC MATERIALS

A.Meghea, I.Demetrescu, I.Rau, and D.Ionita

University "Politehnica" of Bucharest – Faculty of Industrial Chemistry Str. Polizu 1, 78126 Romania; E-mail: <u>i_demetrescu@chim.upb.ro</u>

INTRODUCTION: The degradation of metals and alloys used as surgical implants is usually a combination of electrochemical and mechanical effects. Titanium is well known as metallic biomaterial in orthopaedics and odontology, having chemical inertia and mechanical resistance [1,2], being one of the best in the field.

The properties of titanium and titanium alloys passive films and their stability in Ringer 2 solutions are studied in this paper using chemiluminescence, infrared spectra and atomic absorption in order to complete electrochemical methods in the evaluation of implant behavior. [2]

MATERIALS AND METHODS:

The specimens were made from Ti, Ti6Al4V and Ti 6Al2, 5Fe.

The composition of titanium electrode is: 0.056% N₂; 0.015%Fe; 0.205%O₂; 0.015% H₂; 0.09% Al; Ti rest. The composition of alloys is 0.08%C; 0.05%N₂; 0.015%H₂; 0.02%O₂; 0.03%Fe, 6.7%Al; 4.5%V: Ti rest ,and 0.08%C; 0.05%N₂; 0.015%H₂; 0.02%O₂; 6.5% Al; 2.5%Fe; Ti rest respectively.

The electrodes were abraded first of all with emery paper, degreased in boiling benzene, chemically polished in 3% HF+20%HNO₃ for 3 minutes, and then thoroughly rinsed with tap and distilled water

The experiments were performed in Ringer 2 solution, at 37°C, taking into account that this is the normal temperature of the human body. Composition of the Ringer 2 solution is the following: NaCl 0.3 g/l, KCl 0.37 g/l, NaHCO₃ 2.44 g/l, MgCl₂.6H₂O 0.203 g/l, MgSO₄.7H₂O 0.123 g/l, Na₂HPO₄.12H₂O 0.07 g/l and NaH₂PO₄.H₂O 0.069 g/l. The pH is 7.4. It is to point out that the Ringer 2 solution is that with phosphate, this anion having a special effect on titanium film stability.

The experiments were performed using the following techniques:

• IR spectra FTIR JASCO 620 equipment was the instrument for the structure changes.

- Atomic absorption spectroscopy AAS 6 Vario with flame for ion release identification.
- Determinations of antioxidant activity of bioliquid by chemiluminescence.
- X- ray photoelectron spectroscopy using ESCALAB MK II.

RESULTS AND DISCUSSIONS:

Regarding the corrosion mechanism, in the case of Ti and titanium alloys, the good corrosion resistance is the result of formation of very stable oxide, typically TiO_2 , the most stable oxide of titanium. The passive film is a mixture of oxides, but X-ray photoelectron spectroscopy demonstrated that the predominant species is the TiO_2 , as could be seen from fig.1, where the photo emission spectrum of Ti6Al4V electrode in Ringer 2 is presented.

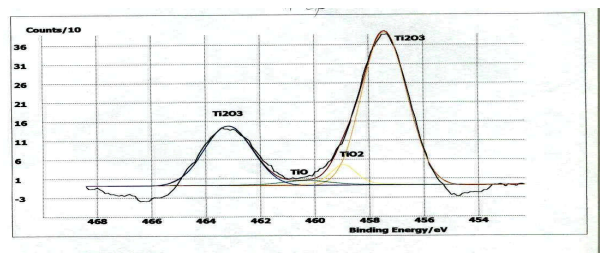


Fig 1. X- ray photoelectron emission spectrum of Ti6Al4V electrode in Ringer 2

The evaluation of the spectra was based on the peak parameters, according to literature data .[3] The TiO₂ formation is evidenced place at 458.94 eV bonding energy. It is to point out that no vanadium oxide was put in evidence, and the presence of aluminum is due to Al⁺³. A value of 71.2 denotes the oxide formation at the external surface of the electrode. All the titanium oxides are in the internal part of the surface in the vicinity of the metal and are responsible for the high corrosion resistance.

In spite of the very good properties, these passivating alloys can generate metal ions, which diffuse through the passive oxide films. First of all the titanium ion release was put in the evidence for the studied electrodes and the evolution of the titanium quantity is presented in fig 2 together with the regression equation of the process.

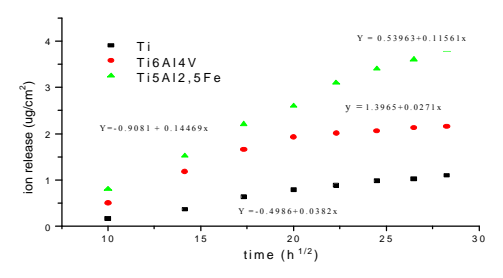


Fig.2. The evolution of titanium ion release in Ringer 2 solution

The initial event during the immersion of titanium in bioliquids is the hydrolysis of the oxide and the establishing of surface-solution equilibrium. Therefore, the passive dissolution is determined by the hydrolysis in the first step. The second step is the transport of dissolution products to the bulk electrolyte. This is a molecular diffusion rate-determining step. The dissolution products released are either neutral species like Ti(OH)₂ or hidroxocomplex such as TiO(OH)₂ [4].

It can be shown why Ti in Ringer 2 solution provides a less susceptibility to corrosion in comparison with Ringer 1 solution [3], probably due to (H_2PO_4) adsorption. In this case, repassivation is the fast step, in the presence of phosphate ions being adsorbed at metal-oxide interfaces. Phosphate adsorption is also supported by spectral data, according to the following arguments:

- characteristic phosphate band (350cm⁻¹ and 1077cm⁻¹ for bonded phosphate) appears in the IR spectrum of the reaction product on the electrode surface, and in the same time a decrease of 3400cm⁻¹ absorbtion band related to the OH of hydrogen bonding is observed. At 590 and 470cm⁻¹ respectively the existence of Me-OH bond is observed. The $(H_2PO_4)^-$ and $(HPO_4)^-$ adsorption is probably due to a complex formation [4] according to the reaction (1) and (2) respectively: $TiO(OH)_2 + 2 (H_2PO_4)^-$ (aq) $\rightarrow TiO(H_2PO_4)_2 + 2 (OH)^-$ (1) $TiO(OH)_2 + aq) \rightarrow TiO(H PO_4) + 2 (OH)^-$ (2) Antioxidant effect of Ringer 2 solution is

Antioxidant effect of Ringer 2 solution is confirmed by chemiluminescence data (fig.3) where the chemiluminescent signal evolution after various immersion time of a titanium electrode is presented.

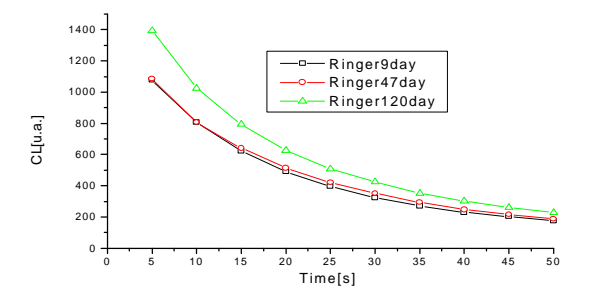


Fig 3. Evolution of chemiluminiscent signal in Ringer 2 solution

A change in the solution behavior could be seen, probably related to the passive stratum penetration. In fact, this is an argument for short life radicals consumption (reactive species of oxygen) during complex formation.

CONCLUSION: Chemiluminescence, infrared, photoelectron X-ray, and atomic absorption spectroscopy are valuable arguments for a better understanding of Ti behaviour in body fluids.

REFERENCES:

- 1. Van Noort, R. J., Materials Science, 1987, 22, 3801-3811
- 2. Demetrescu, I., and Popescu, B., 'Electrochemical behaviour of implant biomaterials', in Electrochemistry and Corrosion, Ed. Printech, 2002, 149-227
- 3. Milosev, I., Metikos-Hukovic, M., Strehblow, H-H., Biomaterials, 21, 2103-2113, 2000
- 4. Hanava, T., Asami, K., Asaoka, K., J. Biomed. Mat. Res., 1998, 32, 530-535.

ASPECTS OF METALLIC BIOMATERIALS DEGRADATION IN VARIOUS SIMULATED BIOLOGICAL FLUIDS

Ioana Demetrescu and Belarisa Popescu

Polytehnica University - Faculty of Industrial Chemistry; Str. Polizu 1, 78126 – Bucharest – Romania

INTRODUCTION: Corrosion [1-2] of implant materials is an important aspect of biocompatibility and only the noblest metals (gold and platinum group metals) or the most passive (titanium or chromium) metals have corrosion rates within apparently acceptable levels.

The metallic biomaterials behaviour in bioliquids is a function of many parameters, related to surface preparation and environment specific composition, including the special influence of the chlorine or fluoride anion, [2] or the effect of organic compounds [3]. Taking into account such parameters this paper is an assessment of the behaviour of a range of implant materials, including titanium and titanium alloys and stainless steels

EXPERIMENTAL PART: Specimens were made from Ti, Ti6Al4V and Ti 6Al2,5Fe and stainless steels (V_4AS,V_2AS)

Table 1 Composition of the studied metallic biomaterials

Biomaterials					0	% Wt.				
Diomaterials	Al	Fe	V	C	O	Cr	Ni	Mo	N	Ti
Ti	0.005	0.095	-	0.04	0.056				0.045	rest
Ti-5Al-4V	4.88	0.021	3.72	0.04	0.175				0.0153	rest
				8						
Ti-6Al-4Fe	6.12	3.87	-	0.18	0.26				0.035	rest
Stainless SteelV ₄ AS,		rest		0.03		16.5-18	10.5-	2-2.5		-
							13			
Stainless Steel V ₂ AS		rest		0.03			9-11	-		0.05
Stainless Steel DIN	-	rest		0.08			10.5-	2-3		0.4
14571							13.5			

All metallic biomaterials were used as cylindrical electrodes. The experiments were performed in Hank, Ringer 1, Ringer 2 solutions with and without lactic acid, artificial saliva. The temperature measurements was 37°C, the usual temperature of the human body. The surface was prepared in 2 different ways [5]. The treatment A was the usual cleaning, including chemically polished in 3% HF+20%HNO₃, and the procedure B was a more carefully one, including ultrasonic treatment.

Composition of the bioliquids are:

Ringer 1: NaCl 8,6 g/l, CaCl₂ 0,33 g/l, KCl 0,3 g/l; pH=7

Ringer 2: NaCl 0.3 g/l, KCl 0.37 g/l, NaHCO3 2.44 g/l, MgCl ₂.6H ₂0.203 g/l, MgSO₄.7H₂O 0.123 g/l,

 $Na_2HPO_412H_2O$ 0.07 g/l and $NaH_2PO_4.H$ $_20.069$ g/l. The pH is 7.4.

Hank: NaCl 8g/l, CaCl $_2$ 0,14 g/l, KCl 0,4 g/l, MgCl $_2$.6H $_2$ O 0,1 g/l, Na $_2$ HPO $_4$.2H $_2$ O 0,06 g/l; KH $_2$ PO $_4$ 0,06 g/l, MgSO $_4$.7H $_2$ O 0,06 g/l si glucoza 1g/l

Artificial saliva: KCl 1,5g/l; NaHCO₃ 1,5 g/l; NaH₂PO₄ 0,5g/l KSCN 0,5g/l; lactic acid 0,9g/l The experiments were performed using following techniques:

Open circuit potential measurement: In open circuit experiments curves potential versus time for a short, medium and long time were obtained and simultaneousely the dependence pH-time was recorded.

Linear polarisation test and cyclic polarisation voltametry using VoltaLab21 with VOLTAMASTER electrochemistry software as a procedure of corrosion rate evaluation.(Stern Geary- method)

Cyclic polarisation experiments were performed using PAR 179 with computer interface

Atomic absorption spectrophotometer determinations for ions release identification

Surface analysis type atomic force microscopy with image analysis program for roughness evaluation

A MedCalc program devoted to medical applications was the instrument for the statistical treatment

RESULTS AND DISCUSSIONS: Variations of open circuit potentials reveal, for all studied implant materials, that these potentials are active at the beginning and tend to a constant level, denoting passive, protective, very stable films for long term exposure, therefore, the implant materials present a long-term stability. In all simulated body solutions, the open circuit

European Cells and Materials Vol. 5. Suppl. 1, 2003 (pages 7-9) potentials of the studied materials were more electronegative for the initial period of about 12 exposure days, then and after various period of exposure days (depending of the material) became nobler. These values fluctuated from more electronegative value in the order V₄AS, V₂AS, Ti-6Al-4Fe, Ti-5Al-4V and Ti. This trend is the same in all bioliquids as an argument of the idea that alloying is not a corrosion prevention requirement, titanium being more stable than its alloys. Monitoring of open circuit potential and the use of a statistical treatment program allows to

obtain the scatter diagrams. The help of such diagrams is important for the computing of the regression equation and the prognosis of the potential evolution for longer time than the experimental one.

The corrosion rates were obtained by linear polarisation. From table 1, it results that all tested implant materials present a good resistance for the 8000 hours period, confirming their very good stability.for Ti and Ti alloys in body fluds, as well as the good stability for stainless steels in the same conditions.

Table 2 Corrosion rates (mm/yr) of all studied implant materials in bioliquids surface treatment (A)

		Corrosion rates (mm/yr)							
Biomaterial	Ringer 1	Ringer 2	Hank	Lactic acid 10%	Ringer 1 +lactic acid 10%	Ringer 2 +lactic acid 10%			
Ti	0,0079	0,0001	0,00035	0,048		0,0000013			
Ti-5Al-4V	0,0114	0,000096	0,000095	0,1470					
Ti-6Al-4Fe	0,024	0,00783	O,0174	0.0 156					
V ₄ AS	0,352	0,289	0,304	-	0,284	0,312			
V ₂ AS	0,387	0,295	0,324	-	0,329	0,315			
316L	0,221	0,176	0,195	-	0,198	0,218			

According to these corrosion rates the amount of ion release is small in all cases, but being a contamination, the monitoring is an important aspect of the degradation and was performed in all cases. As an example in fig.1 evolution of ion releas eand regression equations are presented

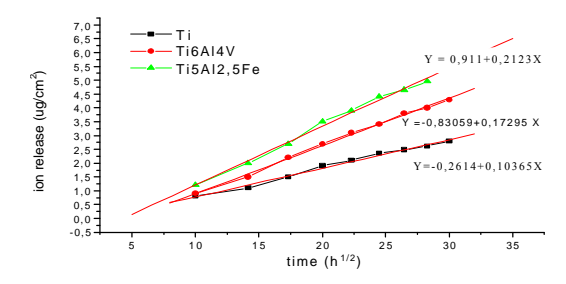


Fig 1. Ion release in Ringer 1.

Polarisation curves and cyclic voltamogrames of titanium and Ti-5Al-4V, Ti-6Al-4Fe alloys obtained after various exposure periods [] show that all biomaterials are self passivated and the corrosion process is under anodic control. The passive films formed on the surface ary stable.

with iron and Ti- allov stainless steel voltammogrames has revealed pitting attack at a pitting initiation potential around 3 V; the hysteresis curve indicates that the cease pitting potential is in all cases around +1.75 V, a very noble potential which can not be reached in the biological liquids. Therefore, there is no risk of pitting attack for this alloy in extra-cellular fluids. In table 3 a measure of susceptibility to local the difference between breakdown corrosion potential (E br) and the protection potential (E pr) are presented for studied implant materials.

Table 3. Parameters from cyclic anodic polarization (surface treatment A)

	$E_{br}-E_{pr}$ (mV)							
Biomaterial	Ringer 1	Ringer 2	Hank	Saliva	Ringer 1 +lactic acid	Ringer 2 +lactic acid		
Ti	-	-	-	130	-	-		
Ti-5Al-4V	2654	800	-	415	100	100		
Ti-6Al 4Fe	2694	1000	1900	-	1520	700		
V ₂ AS	384	332	370	-	358	340		
V ₄ AS	250	217	352	360	225	308		
316 L	232	154	202	373	256	195		

Regarding the surface treatment influence to the corrosion susceptibility, as an example, a Ti-6Al-4Fe electrode sample treated in the way A is compared with a similar electrode treated in the way B, when all the other conditions are similar.

As a result, AFM analysis indicates a 281.4006 nm average roughness, which is correlated with a 1000 mV value (E $_{\text{br}}$ - E $_{\text{pr}}$) for Ti-6Al-4Fe electrodes alloy treated with. 3% HF+20%HNO $_3$. In the case of second sample of Ti-6Al-4Fe

European Cells and Materials Vol. 5. Suppl. 1, 2003 (pages 7-9) electrode, treated in the way B, no breakdown was registered and the average roughness has lower values (194.71 nm).

CONCLUSIONS: In vitro, all tested materials present low corrosion rates which attest their good (stainless steel) and very good stability (Ti and Ti alloys), and this stability is related to environment, and surface treatment and properties.

REFERENCES:

- 1.J. Yu, Z. J. Zhao, L. X. Li ;Corrosion Sci. 35 (1993) 587.
- 2.L.Reclaru and J. M. Meyer; Biomaterials 19; (1998), 85-92.
- 3.R. Born, O Scharnweber, M. Stolzel, M. Thieme, C Wolf, H. Worch, Fresenius J. Anal. Chemistry 361 (1998) 697.
- 4.R. M. Souto, G. T. Burstein: J. Mater. Sci. Material in Medicine 7 (1996) 337.
- 5 I.Demetrescu, B. Popescu, D. Ionescu, Proceedings of EMBEC'02 Viena 2002, 150.

New collagen composites with transdermal application

Ingrid Bujor Ionescu, Viorica Trandafir, Ioana Demetrescu, H. Iovu, Gratiela Zgirian

University "Politehnica" Bucharest – Faculty of Industrial Chemistry Str. Polizu 1, 78126 Romania E-mail: i demetrescu@chim.upb.ro

INTRODUCTION: Collagen polymers have attracted considerable interest for various biomedical applications, including drug delivery system, control transfer therapeutic agents, substrate culture of living cells [1-4]. The physicochemical properties of such polymers are generally designed to be appropriate for their specific function.

The paper is devoted to a preliminary phase of a large research about a new type of composites based on natural polymers with collagen [2], characterized by a trophyc action, which is subject of a patent in preparation. The composite is a collagen matrix with collagen polypeptides bonded with calcium and magnesium ions. This composite is going to be applied as a transdermal dressing and has an effect of fast passing of coetaneous barrier. In this way bioactive components are resorbed by sanguine capillares and reach the general sanguine circulation.

EXPERIMENTAL PART: Collagen membrane is prepared by drying type I collagen fibrillate, in specific condition in order to get micro and nanostructure porous membrane. This structure permits to water vapors to get into membrane by steaming of collagen polypeptide.

• Collagen hydrolysates are obtained by neutral (HO) and acid (HA) hydrolysis of bovine skin at

125°C, 2 atm. for various period of time. After hydrolysis, Ca and Mg salts are introduced, last procedure being atomized drying. The amount of calcium was approximately 10 more than magnesium being around 5 mg/g and 0,6 mg/g respectively.

• The collagen composites are realized mixing atomized powder of polypeptide with collagen fibrillate. Drying at about 28°C is the last final treatment and the porous membrane is the final product.

The composite materials were characterized using the following techniques:

- ➤ Gel chromatography and viscosimetric method for molecular weight determinations
- ➤ Liquid porosimetry with Coulter porometer
- Spectroscopy (UV-VIZ, IR)

RESULTS AND DISCUSSIONS: In order to select an optimal polypeptide size, regarding an easy steaming process, under occlusive dressing, a variety of collagen polypeptide were studied, taking into account average molecular weight presented in table 1.

In this table index value 2, 4, 6, 8 for neutral and acid hydrolysates respectively correspond to the hydrolysis time.

Table 1. The average molecular weight for HO and HA collagen hydrolysates

Collagen hydr	rolysate	Average n	Average molecular weight	
		Viscosimetric method	Gel chromatography	
Neutral	HO ₂	80.700	72.000	> 80.000- 11.500
hydrolysates	HO_4	53.350	62.000	> 70.000- 7.000
	HO_6	20.700	20.500	> 70.000- 3.400
	HO_8	16.250	16.600	> 69.000- 2.900
Acid	HA_2	12.500	15.000	> 70.000 - ≤ 3.000
hydrolysates	HA_4	11.000	11.000	~ 52.000 - ≤ 1.900
	HA_6	9.600	8.800	~ 43.000 - ≤ 1.600
	HA_8	7.050	7.300	~ 43.000 - ≤ 1.400

In table 1 varying hydrolysis time (2, 4, 6, and 8 hours) different polypeptides sizes were obtained, having average molecular weight between 7.000-80.000. It is easy to observe that the average molecular weight of collagen hydrolysates are almost similar from both methods.

Therefore, the polydispersion process is very large, as could be seen from table 1, taking into account the lowest value (~7000) and the highest one (~80.000). The lowest value for average molecular weight in the case of acid hydrolysates being less than 1000, in their compositions there are percentage of free aminoacids.

European Cells and Materials Vol. 5. Suppl. 1, 2003 (pages 10-11) In table 2 physicochemical properties of collagen hydrolysates HO (non atomized) as a function of hydrolysis time. HO_2 with 180000 average molecular weight has a gel aspect and gel process

became over 5% even at temperature around 5°C; HO₄ has a gelatin aspect only at concentration higher then 20%. HO₆ and HO₈ do not present gelatin properties even at very high concentration.

Table 2. Physicochemical values of HO hydrolysate (non atomized)

Physicochemical values of HO hydrolysates	Hydrolysis time (hours)			
	2	4	6	8
Concentration, % g/100ml	22	23	24,6	24,4
pH of solution	8,2	7,8	7,4	7,4
Intrinsic viscosity $[\eta]$ (dl/g) at 20°C, in 0,5 M KCl solution	0,220	0,136	0,071	0,060
The average viscosimeter molecular weight (M _v)	180.000	67.380	20.450	14.800

The atomized hydrolyses present some changes in physicochemical characteristics as could be seen in table 3. The changes are related to a small influence of thermal denaturation of gelatin macromolecules which is take in place at 45-50°C.

Thermal denaturation in the atomize process is more specific in the case of fibrillate protein than in the case of the globular protein. In fact, at a higher degree of hydrolysis the influence on the average molecular weight decreases.

Table 3. Physicochemical values HA and HO hydrolysates (atomized)

Physicochemical values	Hydrolysis time (hours) for			Hydrolysis time (hours) for				
	H	A hydrolysa	te (atomize	d)	HO hydrolysate (atomized)			ed)
	2	4	6	8	2	4	6	8
Humidity, %	3,90	3,73	3,28	3,78	5,15	5,65	4,7	5,6
Total Nitrogen, %	17,27	17,35	17,24	17,51	17,8	17,50	17,67	17,75
Nitrogen from amino group %	0,97	1,12	1,24	1,64	0,61	0,625	0,65	0,75
Total Nitrogen	17,80	15,40	13,90	10,67	29,3	28	27,10	23,60
Ratio (RNH ₂)								
Nitrogen from amino group								
Hide substance, %	97,05	97,50	96,88	98,40	100,05	98,33	99,30	99,75
Ash,%	0,70	0,97	0,72	0,68	0,37	0,53	0,66	0,15
Intrinsec viscosity [η] (dl/g) at	0,055	0,0528	0,0480	0,0408	0,145	0,116	0,0715	0,063
20°C, in 0,5 M KCl solution								
The average viscosimeter	12.500	11.000	9.600	7.050	80.700	53.350	20.700	16.600
molecular weight (M _v)								

Two types of collagen hydrolysates (HO_2 and HA_4) were selected, a neutral and acid one, and Ca and Mg between 0,5-1 % collagen polypeptide.

UV and IR hydrolysates films spectra show that Ca and Mg are banding at carboxyl groups of polypeptide. Electrostatic bond are the indicated one to assure a better ions assimilation and metabolisation into the body.

The composite formation is a three-dimensional fibril structure with pores dimensions between 5-100 nm, for 90% and 0,1-2,5 μ for 10% structure respectively.

CONCLUSION: New type of collagen porous membrane composites with calcium and magnesium were designed and characterized. These composites have a micro and nanostructure, and transdermal applications. Specific area of such a structure is $8 \text{ m}^2/\text{g}$, and permits water absorption and the transdermal transport of bioactive polypeptide .

REFERENCES:

- 1. C. A. Scotchford, M. G. Cascone, S. Downes, P. Giusti: Biomaterials 19 (1998)1-11
- 2. S.D.Gorham: Collagen as a biomaterial In Byron D, editor. Biomaterials, novel materials from biological sources. Basingstoke, Macmillan 1991, 57-121
- 3. H. Iovu, Ingrid Ionescu Bujor, Gratiela Zgirian, Ioana Demetrescu; Proceeding of CAS Conference 2002 Vol 1, 295-298.
- 4.I. Mindru, Mihaela Olteanu, L.I. Dehe; V. Trandafir; Revue Roumaine De Chimie, 28, 7, 1983

ELECTROCHEMICAL IMPEDANCE SPECTROSCOPY TECHNIQUE IN PREDICTION OF THE IMPLANT TITANIUM ALLOYS BEHAVIOUR

D. Ioniþã^a A. Santana Lopez^b, J. Mirza-Rosca^b, E. Vasilescu^c, M. V. Popa^c, P. Drob^c, C. Vasilescu^c

^a Politehnica University, Faculty of Industrial Chemistry, Str. Polizu 1, 78126 Bucharest, Romania
 ^bLas Palmas de Gran Canaria University, Despacho 11, Tafira, 35017, Spain
 ^cInstitute of Physical Chemistry, Spl. Independentei 202, 77208, Bucharest, Romania
 Tel/Fax: 004021 312 11 47; E-mail: m_ionescu@chim.upb.ro

INTRODUCTION: The surface oxide film on titanium and its alloys in bioliquids and its play important an role understanding of titanium implant corrosion resistance. It has been reported [1] that the surface film in human body changes the thickness and composition in time. So, simulation of long-term exposure implants using of electrochemical techniques could be a help for in vivo behaviour prediction. As electrochemical impedance spectroscopy (EIS) is a technique for studying the spontaneous passivation of metals in electrolytes, various oxide films on metal surfaces have been characterized by this technique. Despite a high corrosion resistance of titanium and its alloys, in vivo experiments showed accumulation of titanium ions in tissue adjacent to implants

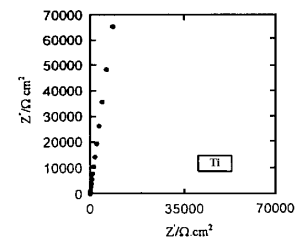
This work investigate the long-term behaviour of Ti and its implant ternary alloys in Ringer's solution of different pHs (6.98; 4.35; 2.5)

EXPERIMENTAL PART: Titanium and its alloys Ti-5Al-4V, Ti-6Al-4Fe were processed into cylindrical electrodes. All measurements were performed in Ringer 2 solution for 12,000 exposure hours. Materials and solution composition were presented in a previous work [4].The following electrochemical techniques were used: impedance spectroscopy, linear polarisation, pH measurements, and open circuit potential. Statistical treatment with Medcalc program was the instrument for the prognosis of the behaviour in time.

RESULTS AND DISCUSSIONS:

EIS data

Impedance spectra, in Nyquist and Bode forms were obtained at open circuit potential and different potentials from the passive potential range.



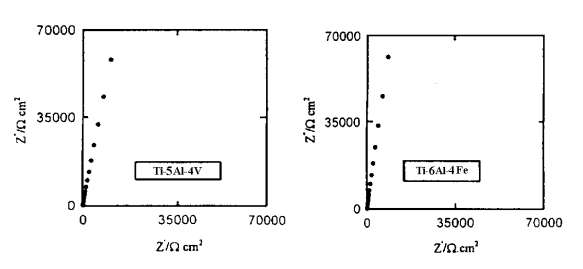


Fig. 1 Nyquist plots at open circuit potential in Ringer's solution of pH = 6.98

At open circuit potential, the impedance spectra (Fig.1) illustrate a pure capacitive behaviour (high corrosion resistance) for Ti and Ti-5Al-4V alloy. Nyquist plots for Ti-6Al-4Fe alloy included a diffusion tail, which suggested that the alloy acted as a porous electrode.

At 0 V, in the passive potential range, Bode plots (Fig.2) exhibit only a near capacitive response illustrated by a phase angle close to -90° over the wide frequency range, indicating a compact, passive film. Bode plots in log |Z| - log f form show linear portions (at intermediate frequencies) with slopes closed to -1.0 (from -0.92 to -0.99). This is the characteristic response of a compact, passive oxide capacitance (C_p). The same Bode plots were obtained at +0.4 V potential, in the passive range, pointing out the same protective film.

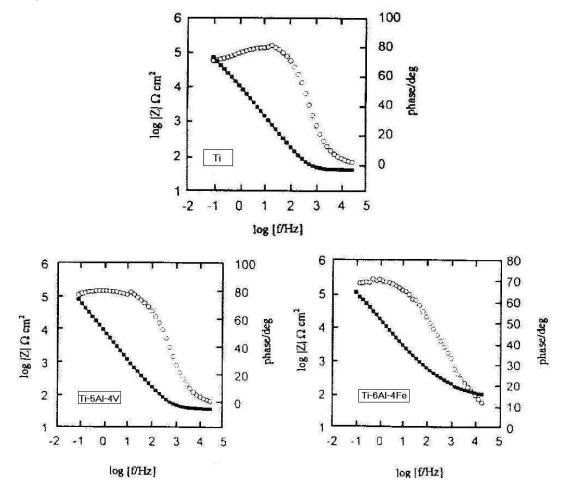


Fig. 2 Bode plots at the potential of 0 V in Ringer's solution of pH = 6.98

The impedance spectra were modelled by fitting these data with an equivalent electric circuit. In the passive potential range, an equivalent circuit European Cells and Materials Vol. 5. Suppl. 1, 2003 (pages 12-14) with one time constant (Fig.3) was fitted for all materials and pHs of Ringer's solutions. The components of this equivalent circuit are: R_{Ω} -ohmic resistance of the electrolyte; R_p – resistance and C_p – capacitance of the passive film.

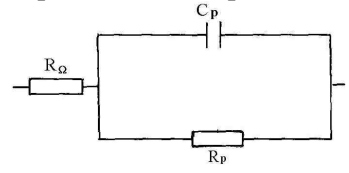


Fig.3 Equivalent electric circuit fitted in the passive potential range for Ti and its ternary alloys

The values obtained for the passive film resistance and capacitance are presented in table 1. It can be seen that the resistance of the passive films for Ti, Ti-5Al-4V and Ti-6Al-4Fe are very high, around 2 $M\Omega.\text{cm}^2$. The very high resistance implies a good corrosion resistance, i.e. a low rate of titanium ion release and the oxide growth. In addition, the passive film capacitance is relatively low, around 15 $\mu\text{F/cm}^2$, and decreases slightly with the potential. This C_p decrease corresponds to a slow growth of the titanium oxide film, indicating a long-term stability of the passive layer.

Table 1 Capacitance and resistance of the film

	Potential		Maaterial	
Paraameter	(mV)	Ti	Ti5Al4V	Ti6Al4Fe
	vs.SCE			
	-800	24	30	46
	-650	27	26	30
C	-500	12	15	22
$(\mu F/cm^2)$	0	14	14	18
	+200	9	12	7
	+400	9	9	11
	-800	0.169	0.221	0.251
	-650	0.039	0.191	0.347
R	-500	-	1.5	1.63
$(M\Omega.cm^2)$	0	0.371	2.07	-
	+200	0.454	1.11	-
	+400	0.212	1.42	1.89

Open circuit potentials for 12,000 exposure hours The open circuit potentials, corrosion potentials (E_{corr}) in Ringer's solution of different pHs for Ti and its alloys decrease in the first 2000 exposure hours, then increase oscillating around $-0.1~V\div -0.3~V$ potential values. These values denote a stable passive film. No pitting corrosion was detected for 12,000 h.

The statistical treatment of the open circuit potential variations in time using the regression procedure permitted the best approximation of scatter diagrams, regression equations and coefficients of determination (table 2).

Table 2 Regression equations and coefficients of determination (D)

Material	pН	Regression equation	D
Ti	6.98	$y=-271.7+0.15x-4.4.10^{-5}x^2+$	0.85
		$4.9.10^{-9}$ x ³ -1.8.10 ⁻¹³ x ⁴	
		$y=-307.9+0.014x-3.91.10^{-7}x^2$	0.73
		$y=-127.76+0.028x^2-2.15.110^{-6}x^3$	0.72
Ti5Al4V		$y=-11611.9-0.002x+3.75.10^{-7}x^2$	0.46
		$y=-291.3-0.02x+1.42.10^{-6}x^2$	0.64
	2.5	$y=-248.6-0.011x+2.4.10^{-7}x^2$	0.84
Ti6Al4Fe		$y=-397.9+0.07x-4.9.10^{-6}x^2$	0.61
		$y=-205.3+0.05x-1.10^{-5}x^2+4.8.10^{-6}x^3$	0.62
	2.5	$y=-321.7+0.01x+4.3.110^{-7}x^2$	0.88

The most important thing in using regression analysis (especially in the cases with a convenient determination coefficient) is the possibility to make some prognosis; in our case, it is a chance to estimate potential for longer time. For example, if in the polynomial equations, the value of time is 15,000 hours, the potential values become close to our experimental values for this time.

It is to point out that in the bioliquids, such predications need more precautions than in other cases, taking into account that the human body being very complex, unexpected phenomenon could take place any time.

Corrosion rates

The corrosion rates of titanium, Ti-5Al-4V and Ti-6Al-4Fe alloys were obtained by linear polarisation for 12,000 exposure hours. From table 3 can be seen that the alloys have lower corrosion rates than the titanium. Both titanium and its ternary alloys have very good corrosion resistance in Ringer's solution at 37°C for 12,000 exposure hours. These corrosion rates will be periodically monitored.

Table 3 Corrosion rates (mm/yr) of titanium and its alloys in Ringer's solutions of different pHs, for 12,000 exposure hours

Material	Time	Corro	sion rate (m	m/yr)
Material	(h)	PH=6.98	PH=4.35	PH=2.5
	2500	4.84×10^{-3}	4.06×10^{-3}	4.96x10 ⁻³
Ti	5000	5.01×10^{-3}	4.22×10^{-3}	5.08×10^{-3}
11	10000	6.12×10^{-3}	5.81×10^{-3}	6.15×10^{-3}
	12000	6.51×10^{-3}	6.68×10^{-3}	6.72×10^{-3}
	2500		3.02×10^{-3}	3.11x10 ⁻³
Ti-5Al-4V	5000	4.25×10^{-3}	3.11×10^{-3}	4.15x10 ⁻³
11-3A1-4 V	10000	5.44×10^{-3}	5.02×10^{-3}	5.88x10 ⁻³
	12000	6.48×10^{-3}	6.59×10^{-3}	6.61×10^{-3}
	2500		3.12×10^{-3}	3.54×10^{-3}
Ti-6Al-4Fe	5000	4.08×10^{-3}	3.21×10^{-3}	4.10x10 ⁻³
	10000	5.42×10^{-3}	5.15×10^{-3}	5.21x10 ⁻³
	12000	6.56×10^{-3}	6.51×10^{-3}	6.69×10^{-3}

CONCLUSIONS:

1. EIS permitted *in situ* characterisation of passive films; impedance parameters indicated a slow

European Cells and Materials Vol. 5. Suppl. 1, 2003 (pages 12-14) growth of oxide layer, corresponding to long-term stability.

- 2. An equivalent circuit with one time constant was fitted for Ti and its alloys in Ringer's solution.
- 3. The open circuit potentials values for very long-term denote a stable passive film; no pitting corrosion was detected.
- 4. The statistical treatment permitted to obtain scatter diagrams, regression equations and coefficients of determination.
- 5. Both titanium and its ternary alloys have low corrosion rates, a very good corrosion resistance in Ringer's solution at 37°C, for 12,000 exposure hours.

REFERENCES:

- 1.J. Pan, D. .Thierry, C. Leygraf, Electrochim. Acta, 41, 1996, 1143
- 2. P. Ducheyne, J. M. Cuckler, J. Biomed. Mater. Res.,31, 1996, 221
- 3. J. J. Jacobs, A. K. Skipor, L. M. Patterson, N. J. Hallab, W. G. Paprosky, J. Black, J. O. Galante, Clin. Orthop., 358, 1999, 173
- 4 M. V. Popa, E. Vasilescu, P. Drob, I. Demetrescu, B. Popescu, D. Ionescu, C. Vasilescu, Mater. Corros., in press

MECHANICAL INVESTIGATION OF A PROXIMAL TIBIAL SLOT DEFECT MODEL

A. Gisep¹, S. Kugler², D. Wahl¹, Ch. Sprecher¹, B. Rahn¹

¹ AO Research Institute, Davos, Switzerland

² Zurich University of Applied Sciences Winterthur, Switzerland

INTRODUCTION: Ceramic bone cements are often used in trauma surgery to fill large defects in comminuted fractures in the near joint area. In an in vivo study¹, the performance and resorption patterns of two different injectable cements (biphasic DCPD - β-TCP and monophasic HA) were investigated in different defects. In a drill hole in the femoral condyles, both cements showed the expected results with different resorption patterns: the hydroxyapatite cement showed minor superficial resorption with good integration in the surrounding bone; the biphasic \(\beta \)-tricalcium phosphate / dicalcium phosphate dihydrate cement revealed a corresponding resorption pattern with faster degradation of the matrix as compared to the granules, which were then surrounded by newly formed bone. In a highly loaded proximal tibial slot defect, cracks started to form in the anterior part, which were immediately filled with new bone. However, the mechanical competence of this situation and the reason for the crack occurrence - mechanically and/or biologically induced – are not known. A mechanical ex vivo test should investigate this question.

http://www.biosurf.ch/

MATERIALS AND METHODS: The tests were carried out on 16 tibiae of sheep with an average age of 60 (31 - 112) months. As implant materials, Norian®SRS® and calcium sulphate dihydrate were used. The shaft of the tibiae was embedded in Beracryl®. The defects underneath the tibial plateaus were created according to Gisep et al., using landmarks (attachment sites of medial and lateral tendons) for the position. The defects were 6 mm high, penetrating about 50% of the a-p depth of the tibia. The posterior cortex was left intact. The bones were divided into five groups: Norian[®]SRS[®] defect filled with 1 2 defect filled with calcium sulphate 3 Norian®SRS®, 1 mm gap on the proximal side 4 calcium sulphate, 1 mm gap on the prox. Side 5 empty defect All mechanical tests were carried out on an Instron 4302 testing machine with a 10 kN load cell. The empty or entirely filled defects were tested in a static mode until failure of the tibial plateau or the cement; the specimens with a gap were tested in a

dynamic manner, 1000 cycles at 1500 – 2000 N. The load was chosen for the tibial plateau to touch the cement surface at every cycle. Crosshead speed in the static test was 1 mm/min, in the dynamic test 15 mm/min. An optical video system was used to measure the real deformations in the defect (Kappa CF 15DSP RGB video cameras with AxioVision Ver. 3.1 software, Zeiss).

RESULTS: The static tests gave the following results:

Table 1. Compression forces taken by empty or entirely filled defects in the static test.

	Defect	Compr. force [kN]
Bone 01	Empty	1.08
Bone 02	Empty	1.05
Bone 03	Empty	1.49
Bone 05	Norian SRS	3.09
Bone 06	Norian SRS	4.10
Bone 08	Norian SRS	3.97
Bone 11	Gypsum	3.87
Bone 12	Gypsum	4.52
Bone 16	Gypsum	2.91

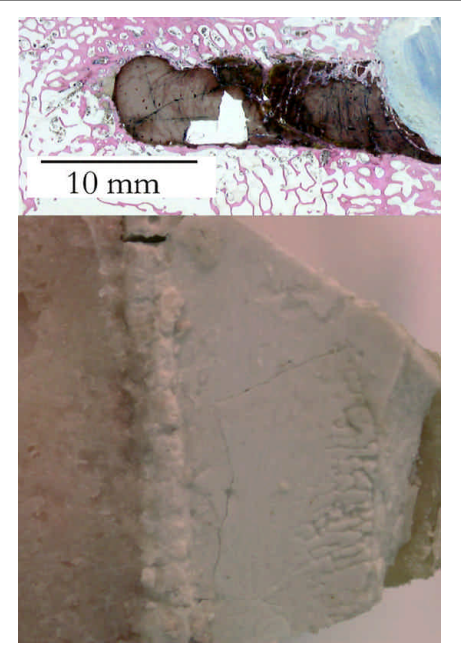


Figure 1. Cracks occurring in the cement after 20 weeks implantation (top, sagittal section through tibial slot defect) and after 1000 cycles in the dynamic ex vivo test (bottom, view on transver-

European Cells and Materials Vol. 5. Suppl. 1, 2003 (pages 15-16) sal plane, top of the implanted cement). Small cracks in the anterior part, large cracks posterior.

The empty defects held forces of 1.21 ± 0.25 kN. Filled with either Norian SRS or calcium sulphate, the average load taken until failure of the bone/cement system was 3.7 kN, which corresponds to about 5 times body weight of the sheep. The optical system revealed no deformations in the defects up to the maximum load, when the cement failed. In the dynamic tests, a similar crack pattern formation could be observed as in the *in vivo* study with only 1000 cycles at loads of 1.5-2.0 kN.

DISCUSSION & CONCLUSIONS: All empty defects failed at loads between 1.0 and 1.5 kN. This load corresponds to less than 2 times body weight of a sheep. This is by far exceeded during a gait cycle on uneven ground, running or jumping². Failure strength of the filled specimens was about 3 times higher as compared to the empty specimens. The dynamic tests showed, that a highly loaded defect with a small gap fails after only a few cycles with much lower loads than the above mentioned. Such a small gap could result from an incomplete filling of the defect or a disturbed balance of bone formation and cement resorption in the initial healing phase of the fracture. Large comminuted intraarticular fractures with a loss in cortical structure and therefore reduced load bearing capacity should be stabilized with metallic implants before the resulting void is filled with ceramic bone substitute materials.

REFERENCES: ¹A. Gisep et al. (2003) Resorption patterns of calcium-phosphate cements in bone, J Biomed Mat Res, accepted for publication. ²GN. Duda et al. (1998) Analysis of interfragmentary movement as a function of musculoskeletal loading conditions in sheep. J Biomech.

CHARACTERIZATION OF IMMUNE REACTIONS TO METALS

W.P. Bieger

ANTOX GmbH, W. Mayer, Immumed GmbH Goethestrasse 4, 80336 München, Deutschland

Metals and their ions are released from dental materials, orthopedic implants, they originate from drugs and vaccines or are inhaled and ingested. Intoxications through environmental or workplace exposure to high concentrations of metals are rare events. In general, metal associated health problems are more related to long-term internal or external exposure to lower, subtoxic concentrations. In recent years mercury has been a major focus of interest and of controversies. By some, mercury is regarded as a major health problem. Another heavy metal, nickel, is unequivocally the number one contact allergen with a sensibilization rate of up to 25% among the female population. Dental amalgam is the major source of mercury, except in fish consuming populations where the lipid-soluble, highly neurotoxic methylated derivative of mercury is the prevailing source. Besides prolonged exposure there are obviously genetic susceptibility factors important in the development of individual intolerance reactions. There is, for instance, increasing knowledge about individual differences in the metabolism and elimination of xenobiotics, toxic metabolites and metals as well. Genetic polymophisms and differences in gene expression result in highly variable activities of detoxification enzymes, some of which - like the glutathione-Stransferases, are also relevant for the elimination of metals. These and other individual factors are determinants of individually different patterns of reaction to otherwise identical metal concentrations. The most relevant determinant of xenobiotic tolerance. even in very low concentrations, is the immune system. It serves as a sensor and filter for all kinds of external materials entering the organism via the respiratory tract, the skin or the digestive system. In animal models many basic principles of immune reactions to metals have been established. For mercury in particular a comprehensive concept of the immunological reactions leading to the autoimmune glomerulonephritis in genetically susceptible rodents, has been established and the potential self antigen fibrillarin has been identified. But these and other results of animal studies on metal intolerance may not be relevant to humans. Thus mercury while provoking non-organ specific autoantibodies obviously does not induce autoimmune diseases in humans and a mercury-specific autoantigen has not been identified. In-vitro two completely different types of immune reactions to mercury can be distinguished. Higher, supranormal concentrations of metals induce cellular stress reactions, characterized by the generation of free radicals and a profound drop in mechanisms. antioxidative defense Consecutive destabilization of the cellular redox balance results in an inflammatory type immune reaction via activation of NF-kB related, redox-sensitive transfer factors. Among

the NF-kB dependant reactions are the increased expression of heat-shock proteins like Hsp 70, and of the TH1-type pro-inflammatory cytokine interferon gamma. Metals/metal ions like titanium that are water insoluble may induce that type of particle-dependant inflammatory response. Finally, in genetically susceptible patients low concentrations of metal ions can induce metal hapten-specific T cells and an interleukin 2 triggered proliferative cellular immune response of delayed type, a type IV allergy. The probable carrier molecules forming a complete antigen with the metal hapten have not been identified so far. The specific type of cellular immune reaction to metals is not suitable as a general tolerance test since it will only be established after exposure to the particular metal. Although the knowledge of the frequency of delayed type immune reactions to certain metals can be of help. The unspecific inflammatory immune reaction to metals on the other hand could serve as a valuable invitro technique in establishing the biological tolerance threshold for metals in humans. For this purpose our group has developed an in-vitro test system for the characterization of individual xenobiotic tolerance thresholds. This so-called Immune Tolerance Test (ITT[®]) has enabled for the first time the diagnosis of multiple chemical sensitivity (MCS) by in vitro exposure of patient lymphocytes to low concentration test chemicals. The established test procedures for type IV allergies are the patch test and as in vitro test the lymphocyte transformation test (LTT), both with specific advantages and also some drawbacks. The skin tests are prone by the prevalence of unspecific irritative reactions, the chance of test-induced sensitization and lack of specificity for a number of chemicals including metals. The LTT has been greatly improved in recent years. A new, highly specific and sensitive version of the test has been developed by our group, called LTT-**CITA**[®] (Cytokine Improved Transformation Assay) and has been introduced for the assay of xenobiotic allergies in general and metal allergies in particular. It has proved its value also for protein antigens from food, bacteria, viruses or moulds.

The individuality of the cellular immune response to chemical antigens can be further dissected by characterizing the effector response in vitro at the level of cytokine gene expression, allowing a high throughput and fast way of testing (Effector Gene Test). Cellular immune reactions to metals may either belong to the Th1 type with interferon-gamma being the prominent cytokine expressed after incubation of the lymphocytes with the antigen or to type Th2 with interleukin 10 as the major reactant. If interleukin 2 is also expressed a broad proliferative response to the particular antigen can be expected, resembling the specific delayed-type immune reactivity.

CLINICAL APPLICATIONS OF METAL ANALYSIS

Georgetta Tapparo and Ottaviano Tapparo

D- 81669 München Rosenheimerstr.46

The discussion about the effect of metals on the organism is still discussed controversial. Metals can cause toxic or allergic reactions. The role of certain metals as Cadmium and Nikel in neoplasia is accepted today. Every Implant cause a reaction after their introduction. This can be an aposition of tissue called integration or a dissolving which leads to failure.Stil today we are in most cases searching bakterias and dont think about reactions that can be caused by the matial itself. In Orthopedics the implants are close implants whereas in reconstructive dentistry there is a contact between bone and the oral cavity, that means we deal with open implants. In the oral cavity there is a continuous presence of microorganisms, bakteria and oxygen. After placement of an Implant the reaction of the tissue depends on the components released by corrosion too. The corrosin depends on many facts like the surrounding the tissue. how implant manufactured and the time it stays in place. Therefore it is extremely difficult to find a direct cause of disease after the placement of metals . In orthopedics surgical steel tantal titanium or titanium alloys with or without a layer or treated ar used.In dentistry amalgams, non precious, semi precious or precious alloys are often used in the same oral cavity.

Therefore in my oppinion we cannot use for an evaluation the maximal dayly intake dose for workers or the lethal dose in the animal model which was discussed a lot in the amalgam discussion. The first deals with healthy workers,, one substance contact period 5 days 8 hours a day. The second with healthy animals (rats or mice who are able to synthetise vitamin c a potent antioxidant) show the lethal dose which we never find dealing with metal implants. In acute toxicity we have diagnostic parameters and treatment protocols whereas in cronic tocicity the diagnosis is very difficult because in after placement also substances contact the organism. other Hairanalising a measurement method daily used in court shows us the intake of a substance but the concentration rarely correlates symptoms. The test of the saliva after chewing for 10 minutes shows us a corrosion rate but is difficult to reproduce.Data about the normal concentration for metals in tissues are rare. Most authors refer to the work done by Ciba Geygy

1979, Williams 1981 or Merian 1991. Chelating substances and their excreted metabolites are life saving in acute poisoning but also there between seldomexist a correlation concentraciton of the chelated substances and symptoms. (DMPS for the chelation of Hg and other metals and EDTA for the chelation of Pb and other metals). All these tests show us the substances we are in contact with or which are stored by the body. For an ideal clinical diagnosis or therapy we should need to know the individual medical history the genetic predisposition, the interaction of the the different substances,the detoxification capacity, the free radical situation of the organism and the reaction of the materials on the immune system. We can test the detoxification capacity of the liver, the free radicals and the disbiosis or inflamation of the gut but thes tests don't show the specific reaction of a substance.A further important mentioned before is that we deal with alloys and corrosion products. These can trasnsformed by microorganisms and can be more toxic as the initial substance. Very often they are able to pass the bloob brain barrier or the placenta barrier.

For the clinical evaluation it is very important to consider that the nerv system is high in fat where these substances can be stored. That means we deal with a lot of nervous disorders which makes the diagnose difficult.

In our office we now use for specific individual testing for metals and other substances in vitro testing. The cltt-cita is a modified lymhocyte transformation test and gives us better results than the path test. The Effector/gentest is used as a tolleration test for materials we want to use in the future. These tests show us the individual predisposition and beware of failures caused by the materials. We saw implant failures if the implant material or the alloy used for the supraconstruction reacted. Single substances, alloys and also their corrosion products can be tested.In our research in dentistry we showed that every metal used in the oral cavity is deposited in the tissues. If the metals are removed the concentration of the metals in the tissues decrease tremendously (Table metals at:Pb,Cd,Ga,Co,Au,In,Cu,Mo;Pd,Pt,Ag,Tl,Bi,Zn,

Common or specific symptoms related by the patients with intollerance or allergy to metals

European Cells and Materials Vol. 5. Suppl. 1, 2003 (pages 18-19) disappered after remova lof the disturbing material. New research done on tips of teethroots after resections show Formaldehyde Putrescine or Cadaverine in the samples which can probably cause problems in patients with cancer, diabetes or chronic degenerative diseases.

In dentistry they can lead to infection and to implant failure if the implant is next to the inflamated tissue.

If we don't want to have failiures and for a predictable long term success we have to remove these substances wich cause reactions. We claim that the remotion is independent from the capacity to detoxify or eleminate the sbstance. A treatment with Vitamins, Minerals, Aminoacids, unsaturated fatty acids can be a support but does not replace the remotion.

The old principle of toxicology and allergy to remove and to stay away from the sbstance that causes a reaction is still valid.

In vivo comparison of two hydraulic calciumphosphate cements in a drill hole model in sheep

Andrea Oberle¹, Felix Theis¹, Marc Bohner², Jessica Müller¹, Christian Frei³, Ilka Boecken², Jörg A. Auer¹, Brigitte von Rechenberg¹

¹Musculoskeletal Research Unit, Equine Hospital, University of Zurich, ²RMS Foundation, Bettlach, ³ Stratec Medical, Oberdorf

INTRODUCTION: Synthetic bone replacements are used to fill bone defects in orthopedic surgery as blocks, granules and recently also as injectable hydraulic cements.^{1, 2} Especially the latter have an interesting potential due to the possibility to mold its form according to the clinical situation. These types of cements may be distinguished into hydroxyapatite (PHA) and dicalciumphosphatedihydrate (DCPD) (also called brushite cements), which mainly differ in their resorption behavior. While PHA based cements resorb slowly over a period of many months, brushite cements are resorbed faster and thus, are supplemented with the addition of á-tricalcium phosphate granules. The granules provide a nidus or crystallization point for new bone deposition. In this study a commercially available injectable PHA-based cement (Biobon®) was compared to a newly developed brushite cement (chronOS injectTM) placing emphasis on ease of application, biocompatibility and its resorption behavior over time.

MATERIAL AND METHODS: Biobon® and chronOS injectTM were applied into a drill hole defect (8mm in Ø, 13mm in length) in the proximal and distal femora and humeri of 10 female, skeletally mature sheep in a randomized fashion. Each sheep had 3 holes filled with Biobon®, 3 with chronOS inject™ and 2 holes were left empty as controls. The cements were filled into the defects and the tissue was closed after hardening of the cement (Biobon® 3min, chronOS injectTM 12 min). Animals were sacrificed at 2,4,8,16 and 24 weeks after surgery. Macroscopical assessment was followed by preparation of the bone specimens for histology where sections were embedded in plastic sections. Thick or ground sections stained with toluidine blue were used to calculate the percentage of new bone formation, fibrous tissue and remaining cement, while thin or 5µ sections stained with toluidine blue or von Kossa/McNeal served to study cellular reactions within the tissue.

RESULTS: chronOS inject[™] was easier to apply than Biobon®, i.e. it bonded nicely to the adjacent bone matrix, did not mix with blood within the wound area but rather pushed it out of the drill

hole. In addition, the application device of chronOS injectTM was better. At sacrifice inflammation of the adjacent soft tissue was observed in the early specimens at 2 weeks with the chronOS injectTM whereas in Biobon® this was noticed up to 4 months, similar to the controls. In the histological sections, significant differences were seen in cement resorption and new bone formation (P<0.05) such that Biobon® was almost unchanged 24 weeks after surgery with only minor new bone formation within the cement cracks. This was in contrast to chronOS injectTM where already 2 weeks after surgery a small seam of osteoblasts was noticed at the periphery and at 24 weeks almost the entire cement was replaced with new bone. On a cellular level also major differences were found between the two cements, chronOS injectTM was resorbed continuously over time by macrophages, whereas Biobon® was subjected to osteoclast activity. In addition, foreign body cells and active bone remodeling were noticed in the adjacent bone matrix in Biobon®, which was not the case in chronOS injectTM.

CONCLUSION: chronOS inject™ proved to be suitable as bone cement for orthopedic surgery and was superior to Biobon® in regard of biocompatibility, speed of new bone formation and cement resorption.

- 1. **Bohner M, Theiss F, Apelt D, et al.** Compositional changes of a calcium phosphate dihydrate cement after implantation in sheep. *Biomaterials*. 2002; *in press*.
- 2. **Bohner M.** Calcium orthophosphates in medicine: from ceramics to calcium phosphate cements. *Injury*. 2000;31:S D37-47.

TIME-DEPENDENT ADHESION AND MORPHOLOGY OF OSTEOBLASTIC CELLS ON TITANIUM MODEL SURFACES FEATURING SCALE-DEPENDENT TOPOGRAPHY

O. Zinger¹, K. Anselme², P. Habersetzer³ and D. Landolt¹

¹ LMCH-EPFL, Lausanne, Switzerland. ² IR2B, Berck sur mer, France.

³ Institut Straumann AG, Waldenburg, Switzerland.

INTRODUCTION: The biological performance of implantable titanium devices in medicine and dentistry depends critically on their surface topography in the micro and nanometer range [1,2]. In order to obtain precise information about the effects of the surface topography on cell behavior, one should be able to study independently the micro topography (structures larger than 1 micron), the nano topography (structures smaller than 1 micron) and the superposition of both, without changing the chemical characteristics of the surfaces. A preferred approach is the use of model surfaces. To study the interaction of cells with titanium implants, different model surfaces presenting scale-resolved surface topography were fabricated on bulk titanium and tested using human bone-derived cells.

METHODS: First, to produce well-defined titanium microstructures comparable to cell size, electrochemical micromachining through-mask (EMM) was used. Mechanically polished titanium disks were coated with a negative photoresist. This latter was exposed using a standard UV mask aligner and developed to define the initial patterns. Anodic dissolution of titanium through the patterned photoresist was performed in a methanolethanol based 3 M sulfuric acid electropolishing electrolyte cooled at -10°C [3]. To minimize Joule heating, a sample holder cooled from the inside was used and the electrochemical parameters were optimized using a custom potential function [4]. Secondly, submicrometer structures were produced by two different methods: porous anodization and chemical etching [4]. The electrolyte used for the porous anodization consisted of 1 M H₂SO₄ in osmotically purified water at 25°C. The anodization procedure consisted of sweeping the potential at 20V/s from 0 V to 125 V. Chemical etching of titanium was performed according to a proprietary process of Institut Straumann AG (Waldenburg, Switzerland). It involves immersing the titanium workpiece (mechanically polished microstructured) several minutes in a mixture of concentrated HCl and H₂SO₄ heated above 100°C.

The early phase of the cell-implant interactions was studied using a kinetic morphological analysis of adhesion, spreading and proliferation of MG63 cells. These parameters were evaluated after 4 hours, 24 hours, 3 days and 7 days of cell culture. Scanning electron microscopy (SEM) allowed the morphology appreciation of the proliferation of the cells. Immunolabeling of F-actin allowed the visualization of the cytoskeleton of the cells and then the appreciation of the morphology and the organization of cells in function of the underlying surface, as well as the quantification of cell proliferation. Immunolabeling of vinculin allowed the visualization of the focal contacts distribution of the cells in function of the underlying surface and then the appreciation of their adhesion capacity on the tested surfaces.

RESULTS & DISCUSSION: Optimized throughmask EMM of mechanically polished titanium surfaces enabled to produce well-defined microstructures comparable to cell size. Hexagonal arrays of closely spaced smooth hemispherical cavities of 10-100 μm diameters were made reproducibly using computer-controlled dissolution and precise charge control. Porous anodization and chemical etching, respectively, permitted to generate nano topography on flat and on previously microstructured surfaces [Figure 1].

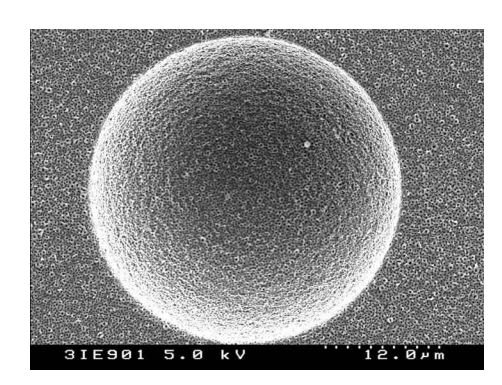


Fig. 1: SEM picture of an anodized titanium surface showing a 30 mm cavity produced by EMM and nanopores resulting from anodic oxidation.(Image courtesy of RG Richards, AO Research Institute, Davos)

European Cells and Materials Vol. 5. Suppl. 1, 2003 (pages 21-23) Thanks to SEM and double immunofluorescent labeling of vinculin and actin, the cells were found to respond to rough nanostructured titanium surfaces by a higher cell thickness and a delayed apparition of the focal contacts. A singular behavior was also observed on the nanoporous oxide, where the cells were more spread and displayed longer and more numerous filopods than on the other nanostructures. On microstructured surfaces, MG63 cells went inside, adhered and proliferated in cavities of 30 μ m and 100 μ m in diameter; whereas they did not seem to react to the 10 μ m cavities [Figure 2].

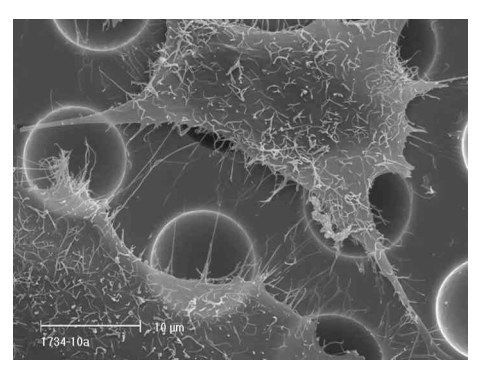


Fig. 2: High magnification SEM picture of MG63 cells cultured 3 days on smooth cavities 10 mm in diameter. Flattened cells covered the cavities, as they did not recognize them as a significant relief.

The threshold in response between 10 and 30 μm diameter cavities could be related to the size of the cells. Condensation aspects of actin cytoskeleton on cavity edges associated with vinculin-positive focal contacts were observed on all microstructured surfaces. Furthermore, cells adopted a 3D shape when attaching inside the 30 μm diameter cavities only, probably due to the curvature of the surface. Nano topography, chemical etching or porous anodic oxidation, superposed on 30 μm micro topography had little effects on cell morphology compared to flat nanostructured surfaces [Figure 3].

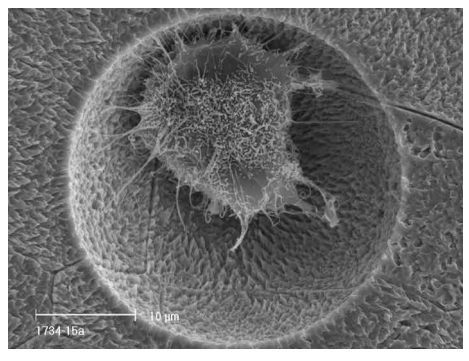


Fig. 3: SEM picture of an MG63 cell, after 3 days of culture, found inside an etched cavity 30 mm in

diameter. The cells adopted a 3D shape when attaching inside the 30 µm diameter cavities only, these latter being smooth, etched or anodized

However, a synergistic effect of nano and micro topography was observed in cell proliferation when combining nanoporous anodization and 30 μ m cavities [Figure 4].

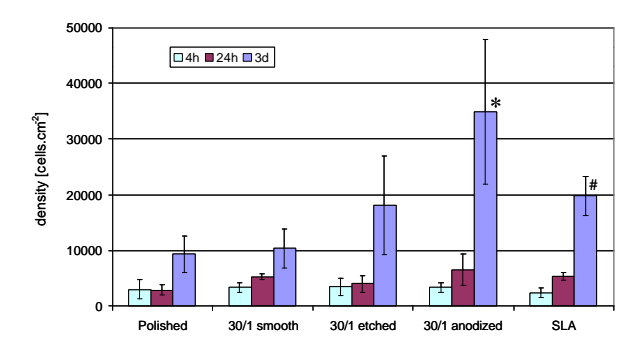


Fig. 4: Cell density on Polished, 30/1 smooth, 30/1 etched, 30/1 anodized and SLA surfaces, after 4 hours, 24 hours, 3 days or 7 days. After 3 days, the cell density on the 30/1 anodized samples is statistically significant compared to all other surfaces tested (marked by *).

CONCLUSIONS: By producing scale-resolved surface topographies on bulk titanium and using selected biological experiments, osteoblast-like cells were shown to respond to surface topography with altered morphology, proliferation and adhesion. More specifically, the behavior of the cells can be influenced differently by nano topography, micro topography or their combination.

REFERENCES: ¹ R.K. Schenk and D. Buser (1998). *Periodontology* 2000; **17**: 22-35. ² B.D. Boyan, C.H. Lohmann, D.D. Dean, V.L. Sylvia, D.L. Cochran and Z. Schwartz (2001). *Annual Review of Materials Research*; **31**: 357-371. ³ C. Madore and D. Landolt (1997) *Journal of Micromechanics and Microengineering*; **7**(4): 270-275. ⁴ O. Zinger, P.-F. Chauvy and D. Landolt (submitted 2003). *Journal of the Electrochemical Society*.

ACKNOWLEDGEMENTS: This work was funded by CTI (Commission for Technology and Innovation, grant number 4719.1) and European Funds for Regional Development (FEDER, Obj.2-99.2-01b-n°78). The thank authors Xanthopoulos (IMX-LMCH-EPFL) for surface analysis, and I. Loison (LR2B, University of Littoral Côte d'Opale) for technical assistance in cell cultures. Institut Straumann (Waldenburg, Switzerland) is gratefully

European Cells and Materials Vol. 5. Suppl. 1, 2003 (pages 21-23) acknowledged for supplying the mechanically polished, etched and microstructured titanium discs; especially J. Luginbühl for titanium dissolution and R. Christ for SEM pictures.

CHARACTERIZATION OF FIBROBLAST ADHESION ON TITANIUM MODEL SURFACES

M. Bühler ^{1,2}, L. Harris ¹, O. Zinger ², D. Landolt ², R.G. Richards ¹

¹ <u>AO Research Institute</u>, Davos, Switzerland.

² Laboratory of Metallurgical Chemistry (LMCH) – Swiss Federal Institute of Technology Lausanne (EPFL) – Lausanne, Switzerland

INTRODUCTION: Studying the morphology and adhesion of cells on different structured metal surfaces can give an indication as to the cytocompatibility of the surface and its suitability for possible further applications on dental or orthopedic implants. The adhesion of soft tissue cells to implant materials can be essential to the success or failure of an implant and is also important for the prevention of infection [1]. Implant surface topography and chemistry are important factors in the adhesion of cells to such surfaces.

METHODS: The substrates tested were Thermanox plastic and titanium (ASTM F67) methods: treated with different mechanical polishing, electropolishing, porous anodic oxidation and through-mask electrochemical micromachining. The micromachined surfaces contained cavities in a hexagonal distribution, either with 10, 30 or 100 um opening diameters. Also three micromachined surfaces with a superimposed porous anodic oxidation were tested (signification "10 smooth" or "10 anod." etc.).

Adjustment of the immunolabeling primary antibody concentration was performed to optimize the labeling of vinculin, an integral focal adhesion protein, allowing quantification of the area of cell adhesion that enabled an assessment of the cytocompatibility of the test substrates. The immunolabelling method described by Baxter [2] was used. Large cell area as well as a high density of focal adhesions are considered to be good indications for soft tissue cytocompatibility [3]. A scanning electron microscope (SEM) served to visualize the labels [4].

On the micromachined surfaces the fraction of fibroblasts growing within the cavities or on the flat surface, as well as how many cells fold over or joined onto the cavity edges or overspread completely a cavity was determined.

RESULTS & DISCUSSION: The morphology of the fibroblasts, showed, qualitatively and quantitatively, that the greatest degree of cell spreading and total cell area was found in cells that

had been cultured on the anodized surfaces [Figure 1].

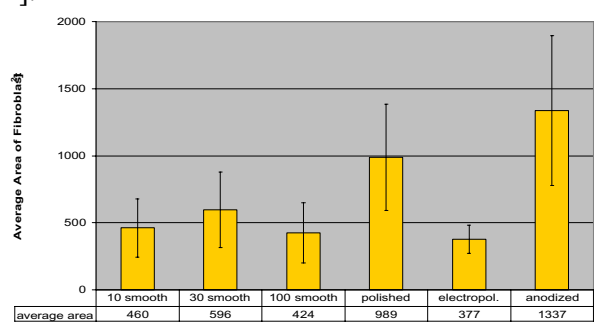


Fig. 1: Average cell areas of fibroblasts grown on different model surfaces.

The areas of cell adhesion for fibroblasts [Figure 2] correlated with the cell morphology results with the greatest amount of adhesion area found on the cells cultured on the anodized surfaces [Figure 3].

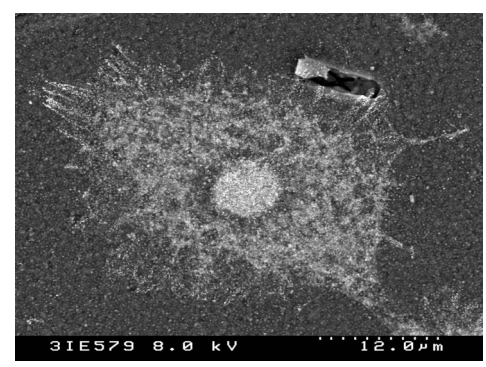


Fig. 2: SEM-image of a fibroblast with gold-labeled focal adhesions from underneath, embedded in resin. Backscattered electrons were detected.

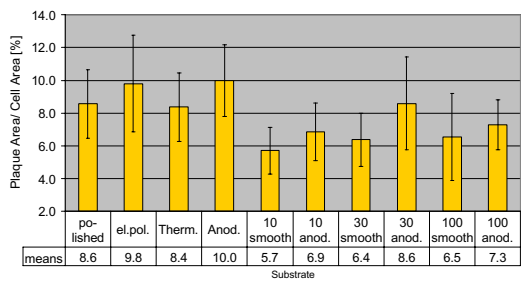


Fig. 3: Ratio of average total adhesion area per cell to the cell spread area.

European Cells and Materials Vol. 5. Suppl. 1, 2003 (pages 24-25)

These results indicated that the anodized titanium with the porous nanotopography would show greater integration of soft tissue when applied to an *in vivo* situation. It was seen that the fibroblasts tend to avoid bending over the sharp cavity edges [Figure 4], whereas they bent over graded anodized edges. The cavities with 10 and 30 µm opening diameter appeared to be too small, so that hardly a cell grew into them [Figure 5].

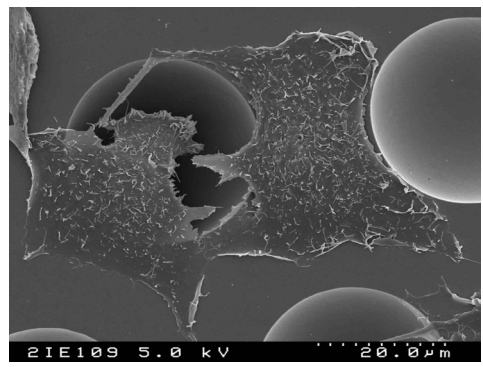


Fig. 4: SEM-image of fibroblasts avoiding to grow into $30 \mu m$ diameter cavities.

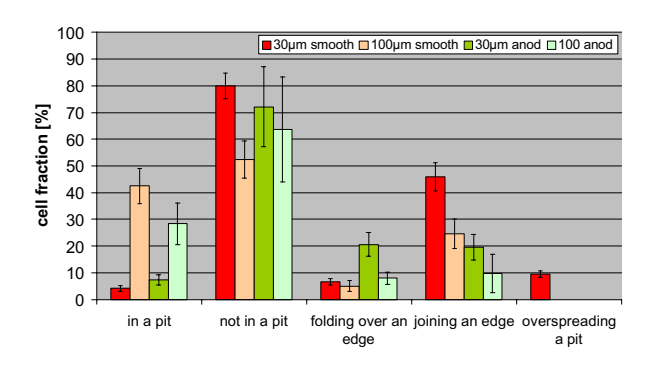


Fig. 5: Distribution of fibroblasts over the different microstructures.

Less than 10% of the fibroblasts grew into a cavity on surfaces with 30 µm diameter pits. About threequarters of the cells settled on the flat parts of this model surface. Much more cells folded over a cavity-edge when porous anodization superimposed over the microstructure. tendency was also observed when counting the cells joining an edge. Instead of joining a cavity-edge, a considerable number of fibroblasts bent over the edges on the anodized surfaces. The ratio of cells joining an edge to cells folding over it (ratio j/f) showed that on graded anodized cavity edges, the cells folded more frequently over them [Table 1].

Table 1: The tendency of cells to bend over a cavity edge.

Surface	30 smooth	30 anod.	100 smooth	100 anod.
Ratio j/f	7.0	4.9	1.0	1.2

The distribution inside and outside the cavities was more equated on the surfaces containing 100 μm pits. The opening diameter of 100 μm appeared sufficient to allow cells to grow in the cavities without limitation. As the total flat surface is equal to the cavity surface, the ratio of cells in and out the pits tended to one.

The lower fraction of cells folding over an edge on the surface 100 μm anodized compared to the surface 30 μm anodized was due to the fact that a lot of cells grew far away from every edge and so the fraction of the totality of the cells folding over is lower.

On the surface with the smallest cavities (10 μ m diameter) no cell grew into a pit. Therefore all cells were influenced in the same way by the presence of these cavities. The fibroblasts grew along the cavity edges avoiding growing into a cavity, and normally overspread one or several cavities.

CONCLUSIONS: The highest adhesion density was observed on the anodized surfaces. The fine nano topography probably induced the cells to produce more focal adhesions. The cavities could have a positive effect *in vivo*, where friction also appears. The fact that more cells bend over the anodized edges indicates that better graded cavity-edges would likely increase the cytocompatibility. It would be interesting to see the effects of cavities on osteoblast cells, which we believe would like the cavities, as this is closer to their *in vivo* situation.

REFERENCES: ¹ Richards RG (1996) *Injury*; 27(3). ² Baxter L, Frauchiger V, Textor M, ap Gwynn I, Richards RG (2002). *Euro. Cells Mat.*; 4: 1-17. ³ Hunter A *et al.* (1995). *Biomaterials*; 16(4):287-295, 1995. ⁴ Richards RG, Lloyd PC, Rahn BA, and Gwynn IA (1993). *J. Microsc.*;171: 205-213.

ACKNOWLEDGEMENTS: The AO Research Institute Davos is gratefully acknowledged for disposing its laboratories and know-how for the immunolabeling method. The Laboratory of Metallurgical Chemistry EPFL is acknowledged for production and characterization of the titanium model surfaces. The authors thank Louisa Patterson and Claire Bacon for cell culturing and Osian Meredith for helpful discussions.

INFLUENCE OF MAGNESIUM ON THE WORKING CHARACTERISTICS OF BRUSHITE CEMENTS

S. Rousseau, M. Buehler, L. Jordi, J. Lemaître

Laboratoire de Technologie des Poudres, EPFL, MX-Ecublens, CH-1015-Lausanne (Switzerland)

The present work aims at adressing some questions raised by a previous in vitro study on the long term aging of brushite cements in simulated physiological conditions. In said study, the following compositional factors were investigated: (A) nature of rheological (hyaluronic additive acid. HA. hydroxypropylmethyl cellulose, HPMC: appr. 1%wt of mixing solution); (B) origin of sulfate ions (plaster of Paris, CaSO₄•0.5H₂O H₂SO₄ diluted in mixing solution; S/Ca = 0.013); (C) addition of magnesium phosphate (0 %wt vs appr 8.5 % wt (D) final $MgHPO_4 \bullet 3H_2O)$, and cement porosity (35 vs 45 %vol). The results have shown that Mg addition increases significantly the degradability of the cements, particularly so in the presence of HA.

Therefore. a more thorough characterisation of these cement formulations has been undertaken: thus, the characteristic working and setting times, the ultimate conversion degree of the cements and their mechanical properties have been investigated. Working and setting times, toghether with ultimate conversion degrees were estimated thermometric analysis technique by developed previously by C. Pittet ¹, based on exothermicity of the consolidation Mechanical properties evaluated by combining uniaxial compression and diametral compression tests. The results have shown that the presence of Mg results in conversion and, lower ultimate consequence, in lower mechanical strength.

In order to highlight the Mg effects, a further thermometric study has been undertaken: in this study, various concentrations of Mg were incorporated in the cement in the form of MgSO₄ dissolved in the

results confirm The specific interaction between dissolved Mg and HA: in the presence of HPMC, Mg addition does not affect significantly the characteristic working times; setting in contrast, these characteristic times significantly are shortened by the simultaneous presence of HA and Mg in the mixing solution. These effects are consistent with the way Mg affects the ultimate conversion degree and the mechanical performance of the cements, which also varies according to the nature of the polymer present in the mixing liquid.

In conclusion, the presence of Mg dissolved in the intersticial liquid present in brushite cements affects significantly their working characteristics, including working and setting times, ultimate degree of conversion and mechanical performances. These effects depend markedly on the nature of hydrosoluble polymers dissolved in the mixing liquid: a specific interaction seems to exist between Mg and hyaluronic acid. It is expected that different Mg-hydrosoluble polymer combinations might result in variable degradabilities and *in vivo* responses.

Acknowledgements

The financial support of the Robert Mathys foundation and of Stratec Medical is gratefully acknowledged. Special thanks are due to Dr M. Bohner ant to C. Frei for stimulating discussion and suggestions.

mixing solution; Mg concentrations were selected so as to represent either 50% or 100% of the saturation concentration of Newberryite (MgHPO₄•3H₂O).

C.Pittet "Development and characterization of injectable calcium phosphate cements for use in vertebroplasty." PhD Thesis work n°2059, EPFL Lausanne, 2001.

FEASIBILITY OF A NEW DUAL-PASTE PRESENTATION OF INJECTABLE BRUSHITE CEMENTS

D. Brendlen, C. Pittet, J. Lemaître

Laboratoire de Technologie des Poudres, EPFL, MX-Ecublens, CH-1015-Lausanne (Switzerland)

This work focuses on injectable calcium phosphate cements (CPC) which, in contrast to conventional hydroxyapatite cements, are converted into brushite (dicalcium phosphate dihydrate, DCPD) as a result of their consolidation processes. The so-called brushite cements are prepared by adding water to mixtures of β-tricalcium phosphate monocalcium phosphate (B-TCP) and monohydrate (MCPM) powders, in such proportions as to obtain flowable pastes. Setting and consolidation occur as a result of dissolution-precipitation reactions inducing the formation of new brushite crystals in de cement paste. As DCPD has higher solubility than hydroxyapatite (HAP) in physiological conditions, brushite cements are expected to show superior biodegradability and faster resorption in clinical applications.

Previous in vivo investigations have shown that brushite cements are promising synthetic materials for the reconstruction of defects ¹, ². bone Compared biocompatible polymeric cements used so far, this inorganic material meets numerous interesting specifications such as: injectability, workability, low heat release consolidation, upon setting, insitu biodegrability, resorbability and osteoconductibility, thus enabling regeneration.

The step of development presented here is related to a brushite cement formulation dedicated to the treatment of parodontic lesions in the dental field. This work aims at achieving a new galenic presentation of ready—to-use cements, consisting in two pre—mixed pastes loaded into a twin—barrel syringe device equipped with a static mixing nozzle.

The study is focused on the working characteristics of the two pre-mixed pastes, namely:

- Their composition, including rheological additives and setting regulators,
- Their rheological properties prior to mixing,
- Their stability on storage after separate loading into a twin–barrel syringe,
- The working properties of the soobtained brushite cements: working and setting times, mechanical performances.

The experience gained so far demonstrates the feasibility of dual–paste brushite cement formulations, showing excellent working properties and good stability on storage for over 6 months.

Future work will concentrate on the long-term stability of dual-paste brushite formulations, and on the effects of sterilisation (-irradiation *vs* autoclaving) on their stability on storage and on their final working properties.

Acknowledgements

The support of CalciphOS SA & Produits Dentaires SA is gratefully acknowledged.

¹ Ohura K., Bohner M., Hardouin P., Lemaître J., Pasquier G., Flautre B., & Blary M. C. "Resorption and bone formation of new β-tricalcium phosphatemonocalcium phosphate cements: an *in vivo* study." *J. Biomed. Mater. Res.* 30, 193-200, 1996.

² Ikenaga M., Hardouin P., Lemaître J., Andrianjatovo H., & Flautre B. "Biomechanical characterization of a biodegradable calcium phosphate cement: Comparison with porous biphasic calcium phosphate ceramics." *J. Biomed. Mater. Res.* 40(1), 139-144, 1998.

RADIOGRAPHIC AND HISTOLOGIC EVALUTATION OF INTRA-ARTICULAR CALCIUM PHOSPHATE CEMENT IN A RABBIT MODEL

<u>Ch. Braun¹</u>, <u>B.A. Rahn¹</u>, <u>R. Wieling¹</u>, M. Fulmer², <u>A. Gisep¹</u>

¹ <u>AO Research Institute</u>, Clavadelerstrasse, 7270 Davos Platz, Switzerland

² <u>Synthes (USA)</u> 1230 Wilson Drive, West Chester, PA 19380, USA

INTRODUCTION: Orthopaedic trauma surgeries often require bone grafting for void filling after comminuted articular fractures, tumor resection or contouring in the cranio-maxillofacial area. Besides autologous bone grafts, there are various possibilities like polymeric or ceramic blocks or granules that can be implanted. In comminuted articular fractures (e.g. Colles fracture) ceramic calcium-phosphate cements are used to support the realigned articular surface. At the application of the viscous cement paste, the material might penetrate into and set as a mass in the intra-articular space. The clinical outcome of this situation is widely unknown.

The present study addressed the issue of intraarticular ceramic calcium phosphate cement in a rabbit model. Parameters like inflammatory reactions, appearance of the cement or direct abrasion of the articular surfaces by the injected cement are investigated clinically, radiologically and histologically.

METHODS: The experiments were carried out in 18 white New Zealand rabbits (age of 17 months) with a weight of 4.4 ± 0.4 kg (permit GR 01/2000). The animals were divided into groups of 3 with observation periods of 1, 4, 12 weeks, and 6, 12 and 18 months. Implantation of the cement was done under aseptic conditions and general anaesthesia. Through a percutaneous approach after a stab incision, a blunt 12 ga needle was introduced into the tibio-femoral joint space. On the right leg, 0.01 ml of Norian SRS Bone Cement was injected through a 14 ga needle via plunger displacement. This amount is equivalent to 0.3ml in a human knee joint based on estimated comparative body weight.

On the left knee, the same volume of ringer-lactate solution was injected with the same approach to the joint space. The incisions were closed with a single suture. Post-operative and 6, 12 and 18 months follow-up x-rays were taken in anteroposterior and mediolateral direction. For the first two post-operative weeks, the animals were kept in single boxes without food restrictions. For the rest of the observation period, all animals were kept in one group on straw. General health was monitored

weekly by the animal keepers. At completion of the observation time, the rabbits were sacrificed with an overdose of barbiturates (Vetanarcol®) given intravenously. Both knees were harvested and fixed in 70% ethanol. Histological processing included PMMA embedding, 200 µm sectioning, macroradiographs and Giemsa-Eosin staining. Light microscopic evaluation was performed on a Zeiss Axiotech microscope with digital image acquisition (Zeiss AxioCam, AxioVision Ver. 3.1).

RESULTS: All animals recovered well within one day of the surgery. Clinically, there were no signs of inflammation of the knee joints: no swelling nor heat generation was detected. The animals were not limited in their movements. On the postoperative xrays, the injected cement was clearly visible in the right knee joint and, in the follow up, no signs of degeneration could be seen. In the contact radiographs of the histological sections, the location of the cement mass could be determined. In 1/18 cases, the cement was found in the lateral aspect of the joint capsule, away from the contact areas of the articular cartilage. In 13/18 cases, the material was detected mainly anterior of the cruciate ligaments and focused on more or less one point in the joint cavity. The biggest mass found was about 3.4x1.4 mm. In 4/18 cases, the material was fragmented and scattered over the whole joint, where as in 3/4 the main content can be found in the posterior region. These findings were independent of the observation

In all cases, the synovial tissues formed layers around the clots from the beginning of the experiment. In the 4 weeks specimens it can be seen how the synovial villi cover the cement and exclude the material from the cavity and its articular surface. Synovial cells were found in cracks in the cement. After 6 months, formation of cartilage and ossification around the material occurs. In the 12 and 18 months specimens, superficial degeneration of the cement by synovial histiocytes can be seen, followed by ossification. At no time can strong, acute or chronic inflammation be detected. No signs of arthritis are seen. The synovial membranes proliferate only slightly in a few cases.

European Cells and Materials Vol. 5. Suppl. 1, 2003 (pages 28-29) Both in the cement injected joints as in the contralateral control side, only moderate deterioration can be found of the cartilage and the cruciate ligaments. Some of these alterations can be definitively determined to be caused by cement. Some of them are most likely caused by the injection procedure itself.

DISCUSSION & CONCLUSIONS: The injected amount of cement did not cause major harm to the articular tissues, joint capsule and cartilage in the rabbit's knee over the observation period of 18 months.

However, the effects of the ongoing ossification and the fate of the newly-built bone substance remain unclear as well as what happens with the rest of the cement.

This should be investigated in a longer follow-up, over as many as 5 years.

ACKNOWLEDGEMENTS: The author wants to thank Synthes (USA) for providing the implant material.

MONITORING OF CELL MIGRATION ON STRUCTURED SURFACES

J.-P. Kaiser and A. Bruinink

MaTisMed, Biocompatible Materials, EMPA, Lerchenfeldstr. 5, 9014-St. Gallen, Switzerland

INTRODUCTION: Cell migration plays a key role in normal physiological processes, such as embryogenesis and morphogenesis and disease. Examples are in wound healing migration of fibroblasts and vascular endothelial cells is essential and in bone healing the migration of mesenchymal stem cells and subsequent differentiation into active osteoblasts. Interaction between cells and implant materials contributes hereby or for certain implants is even a prerequisite for the clinical success (Lauffenburger and Horwitz, 1996¹). An optimal interaction consists in the colonization of the implant surface by the correct cell types and is among others determined by attachment and migration of latter cells. The object of this study was to investigate the migration behavior of cells on differently structured surfaces.

METHODS: For the present studies a fibroblastic cell line (3T3) was used. The movement of fluorescent vital dye (DiI) labeled 3T3 cells was monitored on various surfaces with a confocal laser scanning microscope for two days under cell culture conditions (5% CO₂, 37°C). Each 15 min a picture was taken from previously selected areas of interest. From the obtained pictures the migration pathway and the mean velocity was estimated by special software.

RESULTS: We could show that the vital dye used did not affect cell functionality. Also the CLSM monitoring strategy did not affect the cell migration indicating the correctness of the set-up used to study cell migration on non-transparent surfaces.

On plain surfaces no specific cell orientation in cell shape and migration could be found. On grooved (9.8 μm width, 1.1 μm depth) surfaces the cells oriented themselves along the axes of the grooves. Furthermore, most cells migrated along the grooves. No clearcut orientation of the cells was seen on plain surfaces (Fig. 1).

Computer analysis of each sequence of trajectories (connected line between centres of the same cell in two subsequent pictures) forming the migration pathway of each cell during two days of monitoring, revealed that about 70% of the trajectories were orientated in parallel to the grooves within a variation in the latitude of ± 15 . The trajectory angle distribution was nearly random on plain surfaces.

The topography on the scaffold surfaces influenced not only cell orientation and the direction of migration, but seem also to influence the average velocity of the migrating cells. On the grooved surface more fibroblast cells exhibited a higher migration velocity.

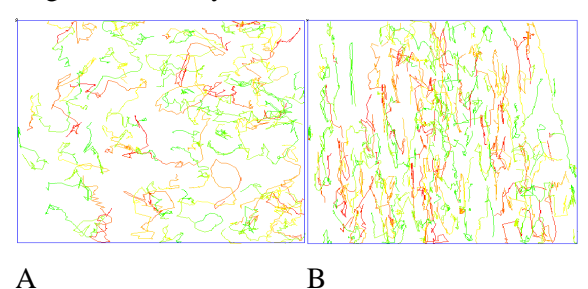


Fig. 1: The two pictures show the migration pathways of the cells cultured on a plain (A) and on a grooved surface (B) during the observation period of 2 days. The migration of the cells on the grooved surface was highly oriented in vertical direction along the axes of the grooves.

DISCUSSION & CONCLUSIONS: generally accepted that micro topography can influence cell shape, cell adhesion, cell orientation, and cell migration. The reactivity to surface structure and chemistry is known to be partly cell type specific (Duncan et al 2002²) and dependent on the groove depth as reported by Curtis and Wilkinson, 1997³. In our investigations the orientation and migration of the fibroblast cells was determined by the grooves. Beside the direction of migration also the velocity of the cell movement was influenced by the topography. Similar observations were reported by Dunn and Brown, (1986)⁴. The present study revealed that the software used represent a easy but powerful tool to analyze cell migration.

REFERENCES: ¹ Lauffenburger and Horwitz (1996) Cell **84**:359-369. ² Duncan et al (2002) Biosensors and Bioelectronics **17** 413-426. ³ Curtis and Wilkinson (1997) Biomaterial **18** 1573-1583. ⁴ Dunn and Brown (1986) Journal of Cell Science **83** 313-340.

EFFECTS OF CULTURE CONDITIONS ON HUMAN BONE (MARROW) CELL PERFORMANCE

M. Hälg, P. Wick, U. Tobler, J. Schug¹, A. Bruinink

MaTisMed, Biocompatible Materials, Swiss Federal Laboratories for Material Testing and Research (EMPA); Lerchenfeldstrasse 5, CH-9014 St. Gallen, Switzerland. 1: Center for Dental and Oral Medicine and cranio-Maxillofacial Surgery, University of Zurich, Plattenstr. 11, CH-8005 Zurich,

Due to the increased life expectancy the need of optimal designed implants is steadily increasing. Since permanent implants have their clear-cut limitations regarding long-term functionality and biocompatibility it is nowadays a general goal in orthopaedics to substitute injured or not functioning tissues (and by that of latter implants) by engineered tissue using cells of the patient.

In case of cartilage and bone tissue engineering osteoblast and chondrocyte progenitor cells have to be cultivated and subsequently differentiated. Current culture conditions are far from optimal.

The present study was undertaken to investigate the role of different medium supplements on cell proliferation and differentiation. In order to be as close as possible to the in vivo implant situation we use human bone marrow (mesenchymal stem) cells of adult patients obtaining a total hip prosthesis.

MATERIALS AND METHODS: Bone marrow mesenchymal stem cells and bone cells were isolated from human femor trabecular bone. Cells were expanded using expansion medium containing fibroblast growth factor, dexamethasone and different sources of serum (fetal bovine serum, FBS, adult bovine serum, BS, or adult human serum, HS; with or without heat-inactivation). At confluency cells were isolated by trypsinization and seeded into well of 24-well plates in expansion medium. After 3 days medium was replaced by medium without additions, by medium with dental extracts [1] or particles (grinded teeth), or by differentiation medium containing âglycerophosphate, dexamethasone ascorbic acidphosphate (with or without vitamin 3OH-D₃). Cell performance was determined by measuring total culture DNA, protein and alkaline phosphatase (ALP) activity.

RESULTS AND DISCUSSION:

Serum effects

Generally, foetal calf serum-containing media are used in *in vitro* experiments. Although cells behave well in these media several aspects must be kept in mind, i.e., that latter addition is rather artificially. Our findings indicate that indeed serum source as well as pre-treatment (heat-inactivation) affect human bone (marrow) mesenchymal cell performance and substratum serum-protein

adsorption (Hälg, 2003). These data support our hypothesis that the choice of serum source and serum pre-treatment may greatly affect the outcome of the cell culture experiments. Furthermore, it could be shown that in case of human serum heat inactivation has an adverse effect on cell yield (Fig. 1). The yield using untreated human serum was comparable to that of FBS.

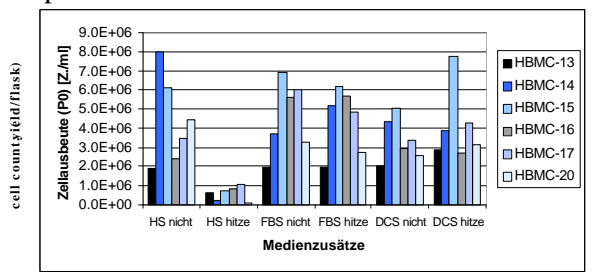


Fig 1. Effects of different sera and serum treatment on the cell yield of adult human stem cells at confluency (before the first passage) in 6 experiments (HBMC 13-17 and 20). Please note that heat inactivation of human serum specifically reduce the yield

Particles

Grinded teeth particles were found to have an adverse effect on human bone cell performance. However acid and guanidine extracts of these particles promote cell proliferation with simultaneous reduction of osteoblast differentiation. Furthermore, remnants of these extracts were found to attract cells.

Acknowledgments. We acknowledge Prof. J. Grünert fort he supply of human bone marrow and Dr. Fopp for the provision of human serum.

References

Hälg M (2003) Einfluss verschiedener Seren auf humanen Knochen(mark)zellen. Diplomarbeit FH Wädenswil/EMPA.

Schlagenhauf U. Mensenchymale Zellen der humanen Zahnpulpa, Beobachtungen und Experimente an einem Zellkulturmodell, in *Medical Faculty*. 1992, Eberhard-Karls-Universit‰t: T, bingen. p. 84-93.

SURFACE TREATMENTS OF TITANIUM IMPLANTS

J.Cl. Puippe *INNOSURF*

Innovation Center of the Estoppey-Reber Group

Electrochemical and chemical surface treatments of titanium and titanium alloy implants include passivation, colour anodizing, alkaline "grey" anodizing, and electropolishing. The latter can be applied as a final treatment or prior to anodizing.

The main purpose of the electrochemical surface treatment, the colour anodizing,

has been over years the part identification. More and more surface functionalities brought by appropriate surface treatments are expected from the surface of dental and orthopaedic implants. The surface should warrant a good corrosion and wear resistance, anti-galling properties as well as an optimal biological response.

"The development of new surfaces can improve the overall performance of titanium implants, particularly in regard to the acceptance of the device by the body, the healing time after implantation and the long term integrity and stability of the biomaterial/body interface." [1]

Chemical and electrochemical surface treatments are well appropriated to modify the surface topography and to control the chemical composition of the outmost layer that plays a relevant role on the biological performance of the material.

Different surface processing methods are described in ref [2]. The chemical and electrochemical processes offered by Innosurf are briefly described hereunder:

PASSIVATION

Passivation treatments provide a controlled and uniformly oxidized surface state. The passivation leads to a dense and stable oxide film and improves corrosion resistance (decreases ion release). The passivation procedure involves nitric acid eliminating metallic contaminants from the surface. It has however practically no influence on the overall surface topography of titanium surfaces. The resulting layer of this chemical treatment is a TiO_2 film in a thickness of two to six nanometers.

BIOCOAT

(colour anodization)

By this process titanium is immersed into an electrolyte and connected as an anode leading to the formation of an oxide film at the surface

$$Ti$$
 \Rightarrow $Ti^{2+} + 2e^{-}$
 $2 \text{ H}_2\text{O}$ \Rightarrow $2 \text{ O}^{2-} + 4 \text{ H}^+$

$$Ti^{2+} + 2 O^{2-}$$
 \Rightarrow $TiO_2 + 2 e^{-}$

The TiO_2 layer is highly resistive and the oxidation reaction will stop when the applied voltage is equal to the ohmic drop in the oxide film. The thickness of the oxide film is therefore a function of the applied voltage. This function is more or less linear and corresponds to 1.5 to 3 nanometers per applied volt. The proportionality constant depends namely on the alloy material, as well as on the electrolyte composition and temperature.

The oxide film acts as an interferential filter leading to beautiful colours varying in the same sequence as the rainbow when the voltage is increased. Typical thicknesses are in the range of 30 to 300 nanometers.

Biocoat applied directly and after electropolishing pretreatment

The main purpose of this electrochemical treatment is the part identification. However different topographical contrasts and therefore different surface functionalities can be obtained through mechanical and chemical pretreatments. A chemical etching is usually applied leading to a slight increase in roughness. On the other end a topographical levelling can be obtained when an electropolishing step is applied prior to the Biocoat treatment.

BIODIZE

(alkaline grey anodization)

This process is similar to the Biocoat however the specific electrolyte allows the formation of thicker TiO₂ layers in the range of micrometers. This

European Cells and Materials Vol. 5. Suppl. 1, 2003 (pages 32-33) process has originally been developed for aerospace applications and corresponds to the AMS 2488c specifications. Improved wear and corrosion resistance as well as anti-galling properties are the main benefits of this coating for aerospace applications.

Titanium screws with the Biodize treatment

The alkaline anodization found large-scale applications for the treatment of orthopaedic implants. The advantages of this treatment are the following:

- The characteristic grey colour of Biodize is easily distinguishable from stainless steel
- anti-galling and wear resistance
- high strength to weight ratio, good fatigue properties and excellent corrosion resistance
- increase in fatigue strength of 15-20% due to the homogeneous surface treatment
- no introduction oh hydrogen or hydrogen embrittlement
- coating forms a penetrating layer rather than growth or "build-up" at the surface which results in no dimensional change
- The coating tends to level surface imperfections
- re-anodization is possible without need for stripping the original coating. Bare or machined areas will "heal" over and be indistinguishable from the original
- improvement to surface finish of greater than 50% is attained without special vibratory or burnishing methods
- the coating is continuous and does not flake off in highly stressed areas
- the coating is fully biocompatible to the human body

BIOBRIGHT

(electropolishing)

In this process titanium is immersed into an electrolyte and is connected as an anode leading to the dissolution of the titanium material. The electrolyte allows forming soluble compounds with the dissolved titanium. Furthermore the electrolyte develops a viscous film at the titanium-

electrolyte interface providing a mass transport controlled dissolution reaction rate. Protruding parts dissolve faster than recesses leading to a levelling of the topographical contrast.

Efficient electrolytes based on perchloric acid are known since many years [2]. However, due to the explosive nature of this chemical compound, the process did not find large-scale industrial applications.

Innosurf applies a perchlorate free process, Biobright, where all danger of explosion is eliminated.

The removed layer of titanium is in the range of 5 to 30 micrometers. The thickness of the layer to be dissolved in order to reach a good levelling effect depends on the starting roughness of the material.

Electropolished agraphes with the Biobright process

Another beneficial effect of the electropolishing is the elimination of surface contaminants. Moreover since no hydrogen is involved in the preparation steps and since sharp scratches are levelled off, the fatigue resistance of the material increases.

CONCLUSION

In addition to part identification, the electrochemical and chemical treatments of titanium offer a range of surface functionalities related to modification of surface topography and control of chemical composition of the surface layer.

REFERENCES

[1] D.M. Brunette, P. Tengwall, M. Textor and P.Thomsen; Titanium in medicine; ISBN 3-540-66936-1; Springer Verlag 2001; Chap 5 p. 88 [2] id; Chap 8

A PROPOSAL FOR THE CLASSIFICATION OF PRECIOUS DENTAL ALLOYS ACCORDING TO THEIR RESISTANCE TO CORROSION BASED ON THE ISO 10271 STANDARD

C. Manaranche, H. Hornberger

¹ Metalor Technologies Neuchâtel, Switzerland.

INTRODUCTION: A lot of dental alloys are available on the market. Among these alloys, there are the conventional alloys, the so called casting alloys used without ceramics, the bonding alloys used with high fusing ceramics and the universal alloys used without or with low fusing ceramics. It is important to know the physical and mechanical properties of these materials but also their biocompatibility and their resistance to corrosion. Dental alloys are generally placed in the mouth for many years, they must not induce adverse biological reactions such as gingival swelling and erythema, mucosal pain and lichenoid reactions. Although these troubles are often caused not by the materials itself [1, 2], they can be induced by the metallic ions released during their corrosion. In order to decrease the risks to the health, it is necessary to study the corrosion of the dental alloys. Currently, the ISO 10271 Standard [3], describes 3 different corrosion tests: a static immersion test (chemical corrosion), an electrochemical test and a tarnish test. However, there are no indications yet about the possible interpretation of test results. In this paper, we propose a method to compare and classify the dental alloys in relation to their chemical and electrochemical corrosion results.

METHODS: The material tested are pure metals such as gold, palladium, silver, copper and zinc as well as dental alloys which are commercially sold (see Table 1). 54 different materials have been tested. A minimum of four samples of each material were tested by electrochemical corrosion and a minimum of three in chemical test. The samples were cast and prepared as indicated by the manufacturer and by the ISO 10271. For the electrochemical test, the samples are in the form of disks 11 mm in diameter. They are tested with a potentiostat/galvanostat Voltalab Model 21. For the chemical test, the samples are rectangular with the dimensions 35X10X1.7 mm. The solution used and the operating conditions are described in the ISO 10271. The concentration of metallic ions released is measured by Induced Coupled Plasma Spectroscopy.

Table 1. Atomic composition (\circ / \circ) of main elements contained in tested dental alloys

Alloys	Category	Au	Pt	Pd	Ag	Cu
CONV.	Au-Ag-Cu	250-605	0-75	0-60	115-505	145-315
CONV.	Ag-Pd(Cu)	0-65	0	180-615	240-630	0-230
	Pd-base	10-35	0	700-750	0-65	0-110
	Au-Pt-Pd	650-780	65-95	90-160	0-40	0-6
BOND.	Au-Pd(Ag)	300-620	0	280-505	0-225	0-90
	Au-Pt	800-850	110-120	0	0	0
UNIV.	Au-Ag	420-505	0-100	0-145	200-375	0

RESULTS & DISCUSSION: Gold is known for its very good resistance to corrosion in contrast to zinc which is easily corroded. We propose to compare the electrochemical values obtained on these two pure metals with the ones of dental alloys. The following parameters are taken into account: Erest, Ecrit, Q1, Q2 and Q3. The rest potential (Erest), which is measured after two hours immersion of the sample into the defined solution against the reference electrode without applying potential (Fig. 1). Then increasing voltage is applied and the resulting current density is measured (Fig. 2), which correlates to corrosion rate. The first section shows typically a flat curve, and from a certain point, the critical potential (Ecrit), the current rises quickly. The integration of the polarization curve between certain defined potentials, Erest and E1*, E1 and E2, E2 and E3, produces the parameters Q1, Q2, Q3 (Table 2).

For classification of the alloys, first the different parameters were compared with the two selected references, gold and zinc ,and noted between 0 and 1, the notations of all five parameters were added to the total notation between 0 and 5 (Table 2). After measuring all alloys, one could see that certain composition ranges behave similar, therefore for each alloy category an average note was determined (Fig 3). From these results a classification according to five following classes is proposed: starting with class 1 which is better than the note 5.0, then class 2, 3 and 4 in steps of 0.3 and finally

European Cells and Materials Vol. 5. Suppl. 1, 2003 (pages 34-36)

class 5 below 4.1. According to Metalor standard, an alloy must not be in class 5 to avoid the risk of significant corrosion.

Table 2: A proposal of notation system for a electrochemical classification

Parameter	Gold	Zinc	some alloy m1
	note	note	note
Erest	1/1	0/1	n_1 = (Erest _{m1} -Erest _{Zn})/ (Erest _{Au} -Erest _{Zn})
Ecrit	1/1	0/1	n_2 = (Ecrit _{m1} -Ecrit _{Zn})/ (Ecrit _{Au} -Ecrit _{Zn})
Q1	1/1	0/1	$n_3 = (Q1_{Zn}-Q1_{m1})/(Q1_{Zn}-Q1_{Au})$
Q2	1/1	0/1	$n_4 = (Q2_{Zn}-Q2_{m1})/(Q2_{Zn}-Q2_{Au})$
Q3	1/1	0/1	$n_5 = (Q3_{Zn}-Q3_{m1})/(Q3_{Zn}-Q3_{Au})$
Total note	5/5	0/5	$N_{total} = \Sigma (n_1 + n_2 + n_3 + n_4 + n_5)$

*E1=Erest+300 mV/SCE, E2= Erest+700 mV/SCE and E3=Erest+900 mV/SCE

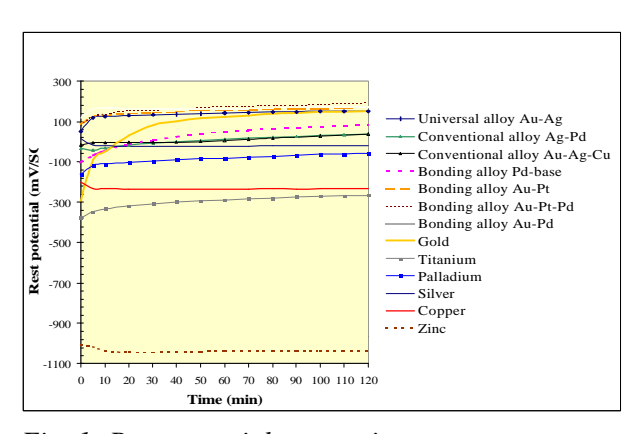


Fig. 1: Rest potential versus time

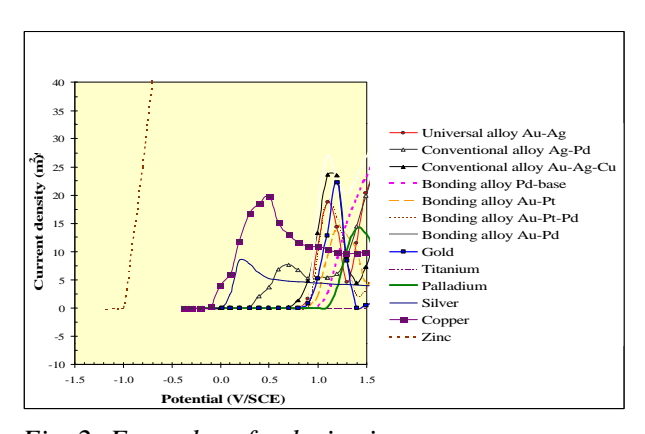


Fig. 2: Examples of polarization curves

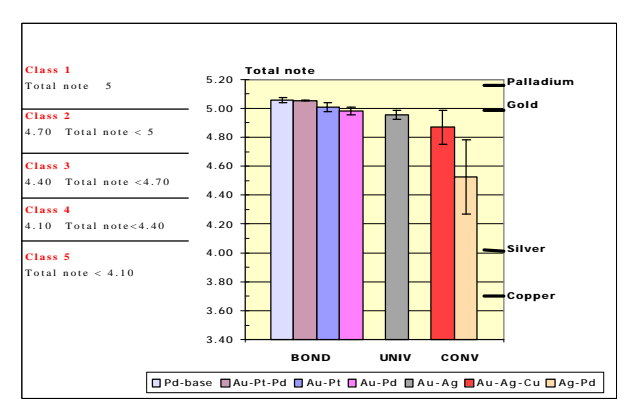


Fig. 3: Electrochemical results

For chemical corrosion the metallic ions released are measured in $\mu g/cm^2$ after one week immersion into the defined solution. The results are calculated as an average for each alloy category (Fig. 4). The classification proposed contains three classes: class 1 up to 10 $\mu g/cm^2$, class 2 between 10 and 100 $\mu g/cm^2$, and class 3 between 100 and 1000 $\mu g/cm^2$.

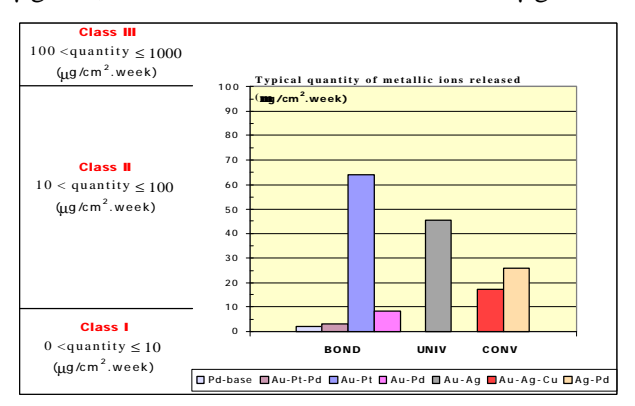


Fig. 4: Chemical results

CONCLUSIONS: In the electrochemical test, the alloys which contain a lot of gold or palladium show a similar behavior as the pure gold and palladium. The conventional alloys contain more silver and copper, they get closer to the values of these metals. In the electrochemical test, typically all alloys were forced to corrode, the values obtained depend strongly on the composition. The corrosion is very significant due to severe conditions (high potentials, aggressive solution). Whereas in the chemical corrosion test, only the phases containing less precious metals were dissolved. This effect can increase strongly when the alloy has an inhomogeneous microstructure or rough surfaces. For these reasons, very good electrochemical results were found for alloys rich in precious metals because it is hard to etch them. As soon as these alloys have a microstructure with several phases they do not necessary have the same classification notes in the chemical test as their homogeneous counterparts.

The Pd-base and Au-Pt-Pd dental alloys are the most resistant to electrochemical and chemical corrosion.

REFERENCES: [1] G. Schmalz, P. Garhammer, *Biological interactions of dental cast alloys with oral tissues*, Dental Materials 18, 2002, 396-406. [2] Environmental Health Policy Comittee, *Biocompatibility of Dental Restorative Materials*, www-health-gov/environment/amalgam1/appendixisectioniii.htm, 1-10. [3] ISO 10271 Standard:

Better scaffolds for cardiovascular tissue engineering; improved mechanical characteristics and better cell attachment realized by precoating of the scaffold.

C.I. Günter*, S. Neuenschwander*, S. Price*, J.F. Visjager·, M. Rahn-Schönbeck , G. Zund*, M.Turina , S.P. Hoerstrup*

* Department of Surgical Research, University Hospital Zurich, © Department of Cardiovascular Surgery, University Hospital Zurich, • Institut of Polymertechnology, ETH Zurich

BACKGROUND:

Scaffolds for cardiovascular tissue engineering must fulfil two conditions:

They have to be pliable into any necessary shape and they should offer an optimal surface for cell attachment, growth and differentiation. Best results are obtained with biodegradable polymers, which mimic the extracellular matrix (ECM) and therefore give the required mechanical stability to the construct, until the newly grown tissue will fulfil this task.

METHODS: We coated biodegradable poly glycolic acid (PGA) with polyhydroxyalcanoates (PHA) 1% and 5% aiming at better mechanical characteristics and improved cell attachment. Human V. saphena magna myofibroblasts were seeded onto the precoated scaffold strips, which were statically cultured for two weeks. Noncoated PGA-strips were used as control.

Cell viability and the amount of cells were estimated with MTT and DNA assays. Hydroxyproline and GAG (glycosaminoglycan) contents was determined in order to characterize the ECM. Finally representative parts of the strips were fixed, stained and examined by light and scanning electron microscopy.

RESULTS: The highest amounts of viable cells were found in the groups of PGA and PGA + 1% PHA as well as the highest total cell numbers and better developed ECM. The histological examinations supported these findings: ECM development and cell ingrowth were higher in the PGA and PGA + 1% PHA groups. The best biomechanical test results were the PGA-strips coated with PHA 5%.

CONCLUSION: Precoating of PGA scaffolds with PHA improves, depending on the concentration used, the mechanical characteristics, cell attachment and tissue formation, therefore this is a promising concept for the development of better scaffolds for cardiovascular tissue engineering.

Keywords: tissue engineering, polymers, myofibroblast

TAILOR-MADE SYNTHESIS OF POLYHYDROXYALKANOATE

Manfred Zinn

Swiss Federal Laboratories for Materials Testing and Research (EMPA), Lerchenfeldstrasse 5, 9014 St. Gallen, Switzerland. Tel.: +41-71-274 7698, Fax: +41-71-274 7788, e-mail: manfred.zinn@empa.ch

The French scientist Lemoigne discovered in Bacillus megaterium inclusion bodies consisting of poly([R]-3-hydroxyalkanoate) (PHB) in 1926 (9). Laboratory studies showed that PHB and other polyhydroxyalkanoates (PHAs) in general are found in combination to a shortage in a noncarboneus nutrient, e.g. nitrogen. When the shortage is relieved, PHA is recycled and used as a carbon and energy source. Since the discovery of PHB more than 90 genera of archae and eubacteria (gram⁺ and gram⁻) have been detected in aerobic and anaerobic habitats able to produce PHA. Only in 1983 PHAs with longer side chains have been discovered (1). To date, PHAs have been separated into 3 classes of PHAs: short chain length PHAs (sclPHA, monomers ranging from C3 to C5), medium chain length PHAs (mclPHA, C6 to C14) and long chain length PHAs (lclPHAs, >C14) (8). Research over the past 20 years focused on the substrate specificity of PHA polymerases. It was found that the supply of bacteria with a particular fatty acid is often reflected in the polymer composition. Thus, PHA monomers with straight, branched, saturated, unsaturated, and also aromatic monomers have been described in literature. Nevertheless only little is known about the chemical and mechanical properties of the polymer because only small amounts of PHA have been produced. Of special interests are functionalized groups in the side chain that allow further chemical modification, halogens, carboxyl, hydroxyl, epoxy, e.g., cyanophenoxy, nitrophenoxy, phenoxy, thiophenoxy, and methylester groups (see also (6, 7). The length of the side chain and its functional group considerably influence the properties of PHA, e.g. melting point, glass transition (flexibility/ and crystallinity temperature, stiffness). The average molecular weight of all PHAs ranges between 10⁵ and 5*10⁶ g mol⁻¹ and is clearly dependent on the microorganism and its growth condition.

Continuous culture studies of microbial growth revealed that PHA-accumulating bacteria are able

grow simultaneously limited by carbon (C) and nitrogen (N) substrates (2-5). It was found that dual (C,N) limited growth is an appropriate method to produce PHA from a toxic carbon source. Since substrate toxicity is dependent on the concentration of the toxic substance, usually growth is not disturbed when the substrate is fully metabolized and, thus, keeping its concentration below a threshold level of toxicity, This beneficial effect of dual (C,N) limited growth of could be shown growth of bacterium with the Pseudomonas oleovorans on n-octane (5).

Recently, it has been proposed that this dual (C,N) limited growth regime offers a new approach to tailor PHA composition during biosynthesis since all carbon substrates were metabolized completely (10). A first test with Ralstonia eutropha (DSM 428) confirmed the concept. Growth limiting concentrations of ammonium, butyric, and valeric acid were fed to a chemostat culture (D = 0.1 h^{-1} , C/N = 17 mol/mol). It was found that the composition of the isolated hydroxbutyrate-co-3-hydroxyvalerate) (PHB/HV) was a function of the carbon substrate mixture. Thus, the content of 3-hydroxyvalerate in PHB/HV could be controlled reproducibly between 0 and 62 mol% (see Figure 1). Interestingly, the polymer composition had a significant influence on the melting temperature and flexibility of the material. In another approach dual (C,N) limited growth (D = 0.1 h^{-1} , C/N = 16mol/mol) was used to tailor functionalized medium-chain-length PHA in Pseudomonas putida GPo1 using 10-undecenoic acid and octanoic acid as carbon substrates. Ten mol% of 10-undecenoic in the carbon feed resulted in the formation of 10 mol% of unsaturated PHA monomers, which allowed subsequent chemical modification.

Concluding, dual (C,N) limited growth offers a new way to produce PHA with tailor-made properties. Current research is focused on the scale-up of the production method.

Figure 1: Tailor-made PHB/HV can be produced in dual (C/N) limited chemostat cultures of Ralstonia eutropha with HV contents between 0 and 62 mol%. The straight line depicts the values for HV in PHB/HV when all valeric acid would be incorporated perfectly proportional to the ratio of butyrate and valerate supplied in the feed. The melting temperature is significantly influenced by the co-polymer composition.

REFERENCES

- de Smet, M. J., G. Eggink, B. Witholt, J. Kingma, and H. Wynberg. 1983. Characterization of intracellular inclusions formed by *Pseudomonas oleovorans* during growth on octane. J. Bacteriol. 154:870-878.
- 2. Durner, R., B. Witholt, and T. Egli. 2000. Accumulation of poly[(*R*)-3-hydroxyalkanoates] in *Pseudomonas oleovorans* during growth with octanoate in continuous culture at different dilution rates. Appl. Environ. Microbiol. 66(8):3408-3414.
- 3. Durner, R., M. Zinn, B. Witholt, and T. Egli. 2001. Accumulation of poly[(*R*)-3-hydroxyalkanoates] in *Pseudomonas oleovorans* during growth in batch and chemostat culture with different carbon sources. Biotechnol. Bioeng. 72(3):278-288.
- 4. Jung, K., R. Hany, D. Rentsch, T. Storni, and Egli, B. Witholt. 2000. Characterization bacterial of new copolyesters containing 3hydroxyoxoalkanoates and acetoxy-3hydroxyalkanoates. Macromolecules 33(23):8571-8575.
- 5. Jung, K., W. Hazenberg, M. Prieto, and B. Witholt. 2001. Two-stage continuous

- process development for the production of medium-chain-length poly(3-hydroxyalkanoates). Biotechnology and Bioengineering 72(1):19-24.
- 6. Kessler, B., and B. Witholt (ed.). 1999. Polyhydroxyalkanoates, vol. 5. John Wiley & Sons, Inc., New York.
- 7. Kim, Y. B., and R. W. Lenz (ed.). 2001. Polyesters from microorganisms, vol. 71. Springer, Berlin.
- 8. Lee, S. Y. 1996. Plastic bacteria? Progress and prospects for polyhydroxyalkanoate production in bacteria. Trends Biotechnol. 14(11):431-438.
- 9. Lemoigne, M. 1926. Produits de deshydration et de polymerisation de l'acide b-oxybutyric. Bull. Soc. Chem. Biol. 8:770-782.
- 10. Zinn, M., B. Witholt, and T. Egli. 2001. Occurrence, synthesis and medical application of bacterial polyhydroxyalkanoate. Adv. Drug Del. Rev. 53(1):5-21.

LINEAR POLYMERIZATION SHRINKAGE OF NEW RESTORATIVE COMPOSITE RESINS

M. Cattani-Lorente, Ch. Godin, S. Bouillaguet and J.M. Meyer

Dental School, University of Geneva

INTRODUCTION: Resin-based dental restorative materials shrink during their setting reaction. Consequently, contraction stresses build up on the cavity walls. As a result, the marginal integrity at the resin-tooth interface may be compromised and a gap formation with subsequent bacterial infiltration may occur [1, 2]. Hence, polymerization shrinkage is a major drawback of composite resins and its reduction is an actual challenge in the dental restorative field.

In the past years, strategies used to reduce the shrinkage were mainly 1) to increase the volume of the inorganic filler incorporated in the composite, 2) to use different co-monomers such as multimethacrylate [3], highly branched methacrylates [4, 5] and ormocers [6], 3) to develop new monomers with low volumetric shrinkage [7], 4) to improve the photo-initiator system.

This last strategy has been recently used by Vivadent and Saremco resulting in the commercialization of two new composite resins (InTenS and ELS).

The aims of the present study were 1) to measure the polymerization shrinkage of two new composite resins and to compare it to the shrinkage of currently used dental composites. 2) to measure the mechanical properties of these materials. The hypothesis tested was that the new initiator systems effectively reduce the shrinkage of the composite resins, without compromising their mechanical properties.

METHODS: Four restorative composite resins: ELS and Trendy Restore (Saremco, Switzerland), InTenS (Vivadent, France) and Herculite (Kerr, Switzerland) were tested.

The device used to measure the free linear polymerization shrinkage was developed by Watts and Cash [8]. A disk-shaped unset composite specimen (ϕ :8mm; h:2mm) was placed on a rigid glass microscope slide, in the middle of a brass ring holding a glass microscope cover-slip of 0.16mm thickness. A LVDT linear transducer (TESA) was placed on the top of the cover-slip and centrally aligned with the specimen. The polymerization was initiated from the bottom of the composite by illuminating the specimen through the rigid glass

slide. A QTH curing unit with an output irradiance of 800 mW/cm², was employed (Elipar Trilight, 3M-ESPE). Specimens were exposed to the light for 60s. The shrinkage data were registered during 30 min with a data acquisition device (Hydra, Fluke). There were five replicates for each material.

The flexural strength and the flexural elastic modulus were determined using a three-point bending test. Rectangular samples of 25x2x2 mm were prepared in Plexiglas molds. The samples were illuminated for 60s on each side with the QHT curing unit. Half of the specimens were light-cured and post-cured for 75s in a laboratory polymerization device (MPa 2000, Columbus) outfitted with a halogen bulb of 400W. All samples were stored at 37°C in water for 24h and tested with an universal testing machine (Instron 1114) at a crosshead speed of 0.5 mm/min.

The filler content of the composites was measured by calcination at 600°C for 3 hours.

The data were compared with a one way analysis of variance followed by a Tukey HSD multiple range test (p<0.05). A t-test was also used to compare the mechanical properties of the composites cured with the two different devices.

RESULTS: Mean linear shrinkage values and filler content for each material are given in Table1.

Table 1. Linear shrinkage (%) and filler content (%) of the dental composites.

Material	Shrinkage	Filler
ELS	1.64 (0.02) a	72.6 (0.1) b
InTenS	1.61 (0.02) a	66.9 (0.4) a
Herculite	2.11 (0.08) b	72.2 (0.6) b
Trendy Restore	1.54 (0.04) a	77.7 (0.3) c

Mean values marked with the same letter displayed no significant statistical differences

There were no significant differences between the linear shrinkage of Trendy Restore, ELS and InTenS. However, these three composites showed significant differences in their filler content.

The flexural strength and the flexural elastic modulus of the composites polymerized with the

European Cells and Materials Vol. 5. Suppl. 1, 2003 (pages 40-41) QHT unit and the laboratory device are given in Tables 2 and 3 respectively.

Table 2. Flexural strength (MPa) of the resin composites cured with the Elipar Trilight and MPA 2000 curing devices.

Material	Elipar Trilight	MPA 2000
ELS	93 (20) a,b	132 (42) b
InTenS	95 (9) a,b	83 (11) a
Herculite	78 (10) a	90 (10) a,b
Trendy Restore	106 (6) b	104 (18) a,b

Mean values marked with the same letter displayed no significant statistical differences

Table 3. Flexural elastic modulus (GPa) of the resin composites cured with the Elipar Trilight and MPA 2000 curing devices.

Material	Elipar Trilight	MPA 2000
ELS	5.5 (1.8) a	11.5 (4.4) b,c
InTenS	6.3 (0.6) a	6.8 (1.0) a
Herculite	7.1 (1.2) a	8.1 (1.0) a,b
Trendy Restore	14.3 (0.9) b	13.9 (1.1) b,c

Mean values marked with the same letter displayed no significant statistical differences

For the post-cured specimens, an increase in the flexural strength and the flexural elastic modulus were observed. This increase was statistically significant only for ELS.

DISCUSSION & CONCLUSIONS:

Previous research has shown an inverse linear relationship between the composite filler content and the shrinkage [9]. Trendy Restore showed the lowest linear shrinkage, which was expected as this composite resin had also the highest filler content. Herculite and ELS had the same filler content, but ELS displayed a lower linear shrinkage than Herculite. InTenS did not show the highest shrinkage value as expected from its filler content. These observations probably indicate that modifications in the initiator system effectively reduced the polymerization shrinkage of ELS and InTenS.

Differences in the monomer to polymer conversion ratio can also account for the observed discrepancy. The degree of conversion was not determined in the present study, as it required a sophisticated equipment. Instead the mechanical properties were measured, because a strong dependence between the extent of curing and the flexural strength or the elastic modulus has been previously established [10]. Moreover, a laboratory curing device with a powerful halogen bulb was used to enhance the cure of the composites. For InTenS, Herculite and Restore, no statistically differences in the mechanical properties were observed between specimens cured with the QHT unit and specimens post-cured. Hence, it can be assumed that the degree of curing of these resin composites was equivalent, whatever polymerization device used. This is not probably the case for ELS, as better mechanical properties were obtained with the laboratory curing device. Consequently, it can be assumed that the reduction in the polymerization shrinkage for ELS is due to a lower monomer to polymer conversion ratio.

In conclusion, modifications of the initiator system can efficiently help to reduce the polymerization shrinkage. The mechanical properties obtained for the ELS and InTenS are superior to those required for posterior restorative materials. The slightly lower elastic modulus of ELS may represent an additional advantage, as some flow of the composite during the polymerization may result in lower contraction stresses at the restoration interface.

REFERENCES:

- [1] AJ De Gee, CL Davidson (1987), *J Dent Res* **66**:1636-1639.
- [2] A Mehl et al. (1997), J Dent 25:321-330.
- [3] CM Chung et al. (2002), *Dent Mater* **18**:174-178
- [4] BM Culbertson et al. (1997), *J Mater Sci:* Pure Appl Chem **A34**:2405-21.
- [5] JE Klee et al. (1999), *Macromol Chem Phys* **200**:517-523.
- [6] H Wolter, W Storch (1994), J Sol-Gel Sci Tech **2**:93-96.
- [7] R Guggenberger, W Weinmann (2000), Am J Dent 13:82D-84D
- [8] DC Watts, AJ Cash (1991), *Dent Mater* **7**:281-287.
- [9] AA Razak, A. Harrison (1997), *J Prosthet Dent* **77**:353-8
- [10] JL Ferracane et al. (1998), *J Biomed Mater Res* **42**:465-472

COMPARISON OF PLASMA MODIFICATIONS (AR/O₂, HE/O₂, N₂/H₂, AND NH₃/H₂) OF POLYSTYRENE CONTROLLED BY XPS ANALYSIS

Xin Gao¹, Ch. Hollenstein², Manfred Schawaller³, and Hans-Jörg Mathieu¹

¹LMCH, EPFL, Lausanne; ²CRPP, EPFL, Lausanne; ³ DiaMed, Applied Diagnostic Systems AG, Cressier.

INTRODUCTION: Polystyrene (PS) is a popular substrate for disposable ware in medical optical diagnostic, primarily due to its transparency, durability, low cost, and good mouldability. As polystyrene lacks reactive functional groups, it is customarily modified by various techniques, such as plasma, gammaradiation grafting or photochemical reactions. Plasma surface treatments are potentially very useful for the covalent incorporation into polymer surfaces of extraneous reactive groups suitable for participation in further, conventional chemical reactions at the surface.² It changes the chemical composition and properties such as wettability, metal adhesion, dryability, lubricity biocompatibility of materials surfaces.³

The purpose of this work is to prepare chemically reactive yet specific PS surfaces for high-density bio-immobilization such as protein molecules. These modified PS surfaces are expected to by applied in medical diagnostic tools for use in a proprietary ADS fluorescence reader.⁴



METHODS: PS chip modification was carried out in a capacitively coupled rf reactor operating at 13.6 MHz. The gas admixture was introduced into the chamber at a flow rate of 60 sccm which maintains the chamber pressure at 0.4 mbar. The plasma was generated at a power of 60 W for 3 minutes. A Scientific System ion flux probe (IFT) has been applied to measure the ion flux on the grounded electrode.

XPS analysis was performed using an imaging Kratos Ultra X-ray photoelectron Axis spectrometer equipped with a conventional hemispherical analyser. The X-ray employed was a monochromatized Al K\alpha (1486.6) eV) source operated at 150 W. Data acquisition was performed under UHV (10⁻⁹ mbar) conditions. Analysis area was 0.21 mm² (300 μ m × 700 μ m) using a take-off angle of 70° relative to the surface normal. Charge compensation was performed with a self-compensating device (Kratos patent) using field emitted low energy electrons (0.1 eV) to adjust the main C-C component to 285 eV.5 The data reduction (atomic concentration, shifting, curve fitting, etc) was performed with CasaXPS Version 2.1.9 software.

RESULTS/DISCUSSION: PS chips are treated with Ar/O_2 , He/O_2 , N_2/H_2 , and NH_3/H_2 plasmas. Ar/O_2 and He/O_2 plasmas are supposed to produce oxygen-containing functional groups while N_2/H_2 and NH_3/H_2 plasmas can produce nitrogen-containing functional groups at PS surfaces.

Table 1 shows the influence of gas mixtures on ion flux and ion doses. A monolayer of PS contains approximately 10^{15} molecules/cm². Compared to the doses values given in Table 1 this means that 10^4 - 10^5 ions/molecule are needed for oxygen- or nitrogen-activation on the PS surface.

Table 1. Parameters for plasma activations^a

Prim. Gas / Sec. Gas (% / %)	Ion Flux (mA/cm ²)	Ion dose (Ions/cm ²)
95 Ar / 5 O ₂	9	1.0E+19
95 He / 5 O ₂	23	2.6E+19
100 NH ₃ /	26	2.9E+19
92 NH ₃ / 8 H ₂	26	3.0E+19
95 N ₂ / 5 H ₂	87	9.8E+19
90 N ₂ / 10 H ₂	95	1.1E+20
70 N ₂ / 30 H ₂	101	1.1E+20

^a Activation conditions: 60 W, 0.4 mbar, exposure of 3 minutes.

In the untreated PS there is no oxygen found. After Ar/O₂ (95/5) plasma treatment, 25 at% O was observed from the survey spectrum, which indicates the introduction of polar O-containing functional groups. Inspecting the C narrow scan spectra reveals functional oxygen containing groups (C-O, C=O, O=C-O, etc) after the plasma treatment (Figure 1). The presence of these Ocontaining functional groups is also confirmed by water contact-angle measurements: Untreated PS has a contact-angle of 83 degrees while after Ar/O₂ plasma treatment, it decreased to 47 degrees, showing an increased hydrophilic surface. He/O₂ plasma treated PS gives similar XPS analysis results as Ar/O₂ plasma treated PS (data not shown).

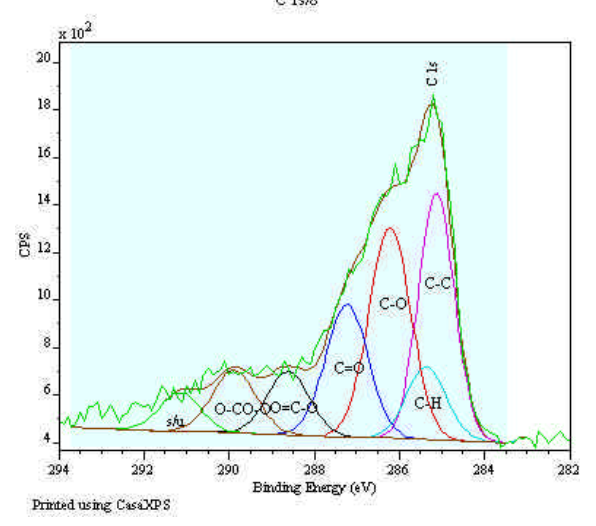


Figure 1. XPS narrow scan spectrum of of PS treated with Ar/O_2 (95/5) plasma.

The efficiency of the plasma activation with N₂ and NH₃ with an admixture of H₂ on PS is checked by nitrogen concentration (at % N) by XPS analysis (Table 2). XPS analysis showed that in the three cases of N_2/H_2 95/5, 90/10, and 70/30 similar surface dilution ratio, modification efficiencies are observed: they give 11±3 at % N. Under the present activation conditions, NH₃ or NH₃/H₂ plasmas are more efficient than N₂/H₂ plasma in providing a nitrogen-amino surface: both NH_3 and NH_3/H_2 (92/8) plasmas give 19 at % N. C1s narrow scan spectrum of PS treated with a NH₃ plasma is shown in Figure 2. It shows the presence of similar CO_x-groups with additional C-N component. Presence of oxygen-containing groups is explained by reaction of the plasma activated surface when transferring the sample for XPS analysis.

Table 2. Nitrogen concentrations of plasma activated PS^a

Prim. Gas / Sec. Gas (% / %)	at % N
95 N ₂ / 5 H ₂	11
90 N ₂ / 10 H ₂	14
70 N ₂ / 30 H ₂	11
100 NH ₃ /	19
92 NH ₃ / 8 H ₂	19

 $^{^{\}rm a}$ Activation conditions: 60 W, 0.4 mbar, exposure of 3 minutes. error: \pm 3 at %

Although the ion dose of N_2/H_2 plasmas is high (Table 1), its efficiency to produce nitrogencontaining functional groups at the surface is lower than NH_3 plasma (Table 2), i.e. that the NH_3 plasma is more effective.

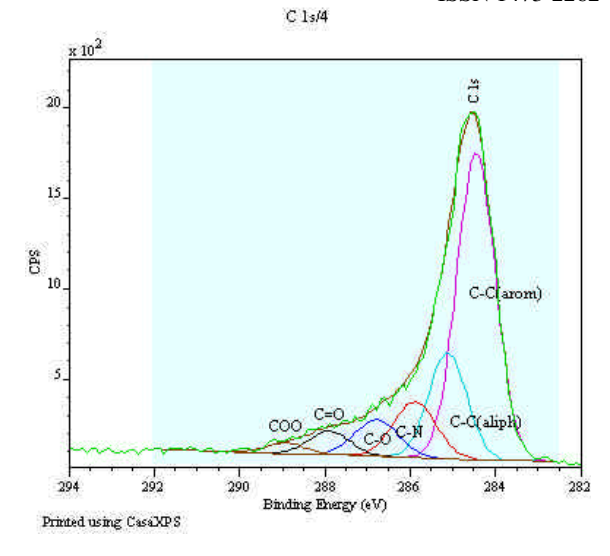


Figure 2. XPS narrow scan spectrum of PS treated with NH₃ plasma.

Conclusions The necessary ion density for PS surface activation is 10^4 - 10^5 ions/molecule per cm². Ar/O₂ and He/O₂ plasmas have similar activation efficiency to give oxygen-containing groups. Admixture of H₂ does not affect nitrogen presence at the PS surface. The NH₃ plasma is almost two times more efficient than the N₂/H₂ plasmas to create active nitrogen-containing sites.⁶

Acknowledgements The authors would like to acknowledge Nicolas Xanthopoulos for assistance with the XPS analysis. The project was financed on a grant no 6142.MTS of the Commission for Technology and Innovation CTI, Bern Switzerland.

Reference

[1] S. B. Idage, S. Badrinarayanan. Langmuir **14** (1998) 2780-2785.

[2] T. R. Gengenbach, X. M. Xie, R. C. Chatelier, H. J. Griesser. J. Adhesion Sci. Technol **8** (1994) 305-328.

[3] P. K. Chu, J. Y. Chen, L. P. Wang, N. Huang. Materials Science and Engineering R **36** (2002) 143-206

[4] patent no. WO 01/14859 A1, EP 1 079 226 A1.

[5] G. Beamson, D. Briggs. *High Resolution XPS of Organic Polymers. The Scienta ESCA300 Database*. John Wiley & Sons Ltd, England, 1992.

[6] X. Gao, Ch. Hollenstein, M. Schawaller, H. J. Mathieu, in preparation.

HEMOCOMPATIBLE DIAMOND-LIKE CARBON (DLC) SURFACES

N. Nurdin¹, P. François², M. Moret¹, K. Unal¹, J. Krumeich³, B.-O. Aronsson¹, P. Descouts¹

¹ Group of Applied Biomedical Physics, Geneva University.
² Division of Infectious Diseases, Geneva University Hospital.
³ Sulzer Innotec, Materials and Surface Engineering, Winterthur, Switzerland.

INTRODUCTION: Diamond-like carbon (DLC) coatings are attractive because of low friction coefficient, high hardness, chemical inertness and smooth finish which they provide to biomedical devices. Silicon wafers (Siwaf) and silicone rubber (Si_{rub}) plates were coated using plasma-enhanced chemical vapor deposition (PE-CVD) techniques. Human blood was used for the in vitro assessment of hemocompatibility. This study has taken into account three events of the blood activation: coagulation, platelet activation and inflammatory process. Tests are based on the observation of platelet adhesion and activation, thrombin generation and complement convertase production induced by the sample surface.

METHODS: Hydrogenated DLC (a-C:H) films were fabricated on Si_{waf} and Si_{rub} using magnetron sputtering techniques with a graphite target and acetylene as reactive gas. Both sides of the samples were coated with a typical thickness of 1μm. Coated surfaces were compared to uncoated materials and to the following reference materials: polymethylmethacrylate (PMMA), polyethylene (LDPE), polydimethylsiloxane (PDMS) and medical steel (MS). The thrombin generation assay (TGA) and complement convertase assay (CCA) were provided by HaemoProbe by as ready-to-use test kits.

TGA can be briefly described as a measurement via an enzymatic colorimetric assay of the amount and the speed of thrombin formation when samples are incubated in a modified plasma. The thrombin generation kinetic for each material is obtained by plotting the thrombin concentrations versus the incubation time.

The complement activation results in the generation of complement factors contributing to the initiation of inflammation process. CCA allows to evaluate the samples for complement factor binding ability.

Platelet adhesion, aggregation and spreading are processes by which platelets form thrombus. Samples were incubated in a freshly prepared human platelet-rich plasma (PRP) according to the method developed by Frank et al [1]. After

incubation, glutaraldehyde was used to fix the platelets on the material surfaces, and imaging was done by scanning electron microscopy (SEM).

RESULTS: Generation of thrombin is the critical event of the coagulation process. Thrombin plays a key role in the formation of blood clot through diverse activities. Figure 1 shows the amount of thrombin generated by the samples in a citrated plasma.

Fig.1: Thrombin generation curves

PMMA, PDMS, MS and Siwaf native surfaces led to the activation of coagulation with a significant increase of thrombin generation after 1 min in contact with plasma. Siwaf was the most activating surface. On this substrate, thrombin generation reached a maximum of approximately 200mU/ml after 2 min of incubation in plasma. For the LDPE and Si_{rub} samples, thrombin generation was dramatically delayed and reduced. These samples did not seem to propagate and amplify the blood clotting process by the thrombin generation event. Thrombin formation was much more retarded in plasma exposed to DLC-coated than to native Siwaf. The time to onset of thrombin generation was about 4min after which an increase to a maximal amount of 174mU/ml was observed. In the case of the Si_{rub} sample, the DLC coating seemed to stimulate a higher thrombin formation than on the native sample. On the other hand, although reaching the same final maximum levels, DLC coatings on Siwaf delayed significantly the induction of thrombin activity and might delay the blood-clotting process.

European Cells and Materials Vol. 5. Suppl. 1, 2003 (pages 44-45) Platelet activation results in platelet shape changes, spreading, aggregation and secretion of their granule content. Platelet surface coverage was very prominent on PMMA and MS, with a strong aggregation (Figure 2). On these surfaces, the platelets were flat and widely spread and seemed to have reached complete cytoskeletal reorganization, with a tendency to achieve complete circumferential and confluent filamentous areas around aggregates. LDPE samples showed platelets with a dense formation of pseudopodia and few developed platelets. Platelets adhered to the Si_{waf} surface to a lesser extent than to PMMA and MS surfaces, but they were in an activated state with the presence of long pseudopodia. In the cases of Si_{rub}, DLC-Si_{waf} and DLC-Si_{rub}, the few adherent platelets remained in discoïd form. Some filamentous areas were observable on the DLC- Si_{rub} surface.

Synthetic surfaces do not only activate the coagulation cascade but do also provoke inflammatory response involving the complement system. PDMS, MS, PMMA, LDPE, Si_{waf} all provoked a complement convertase adsorption whereas DLC-coated surfaces and Si_{rub} sample could be qualified as inactive for complement factor binding (Figure 3).

CONCLUSIONS: DLC coating delayed clotting time and tended to suppress platelet and complement convertase activation, in contrast to PMMA, LDPE, PDMS, MS and Si_{waf} native substrates. The inert nature and the smoothness of the DLC-coated surfaces appeared to dominantly explain the good *in vitro* hemocompatibility.

REFERENCES: ¹ M. Jones, I. McColl, D. Grant, K. Parker, T. Parker (2000) *J Biomed Mater Res* **52**:413-21. ² R. Frank, H. Dresbach, H. Thelen, H. Sieberth (2000) *J Biomed Mater Res* **52**:374-81.

ACKNOWLEDGEMENTS: This work is supported by the COST Action 527 (Contract n° BBW/OFES-NBC01.0051) from the Swiss government, which is acknowledged.

ISSN 1473-2262						
Samples	140μm x 92μm	36μm x 25μm				
PMMA						
LDPE						
MS						
Si _{waf}						
Si _{rub}		4				
DLC-Si _{waf}		-				
DLC-Si _{rub}		-				

Fig. 2: SEM of adherent platelets on samples.

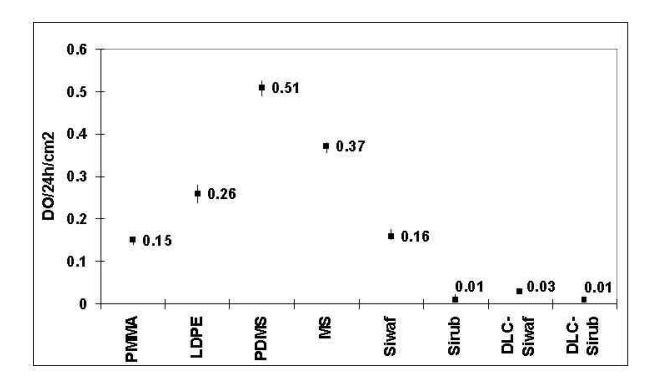


Fig.3:Amount of complement convertase bound to the sample surface.

BIOCOMPATIBILITY AND PERFORMANCE OF AN INTERBODY RESORBABLE FUSION CAGE IMPLANTED IN FUNCTIONAL SITE IN SHEEP

A. Alves¹, J-P. Boutrand ¹

¹BIOMATECH Testing Laboratory, Lyon, France jp.boutrand@biomatech.fr

INTRODUCTION: The aim of the study was to evaluate by histology the performance, the biocompatibility and the degradation kinetic of a resorbable PLA 98 spinal cage following lumbar implantation in sheep.

METHODS: One resorbable PLA 98 spinal cage (Phusiline®, Phusis, France) was implanted per animal between L1 and S1 according to table 1.Undecalcified sections were performed for each implant. Qualitative and semi quantitative histological evaluations were performed.

Table 1: Study design -16 adult sheep

Time	3m	6m	9m	12m	24m	36m
Animal	3	3	2	3	3	2
Implant	3	3	2	3	3	2

RESULTS: After 3 months, early signs of degradation of the cages (fragmentation) were detected. In addition, adaptative changes to the local biomechanical conditions were detected. No signs of osseointegration of the implant were detected at this time period. No signs of resorption were found. Early signs of bone ingrowth in the cage were observed.

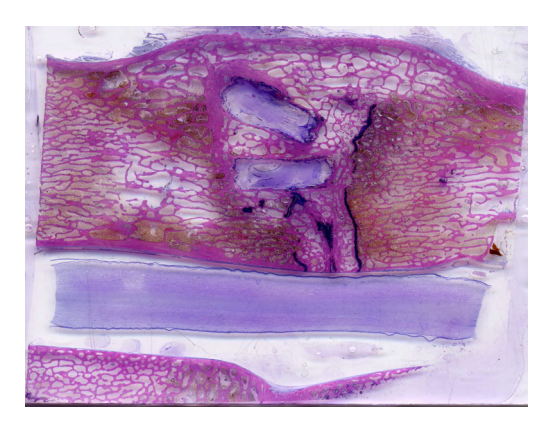


Fig. 1: 24 months: interbody osseous fusion within and outside of the resorbable cage. Major degradation of the implant material with modification of the pH (basophilic affinity to the bluish Giemsa dye) and hollow structures formation (white areas.).Macroscopic picture. Paragon staining.

After 6 months, osteogenesis and bone remodelling around the implant progressed. At this time period

signs of biodegradation and bioresorption were both visible. In some cases, the first microscopic signs of bone fusion were found, mostly around the cages.

Nine months after implantation, fragmentation and erosion of the implants progressed.

Osseointegration was found in several areas of the implant. In 50 % of the cases, microscopic spinal fusion was visible, outside of the cages.

After 1 year, 30 % of the initial implant volume resorbed and was replaced by a trabecular bone. With regard to the implant degradation, cell penetration within the implant was observed. Actual signs of interbody arthrodesis were observed both within (30 %) and outside (100 %) of the cages.

At 2 years, the implant resorption progressed and the implant fragmentation was almost total (Fig.1). Almost 70% of the cases showed osseous fusion within and outside the cage whereas in all cases, bone fusion was observed externally to the device. Three years post-implantation, the remaining implant was totally resorbed and replaced by bone marrow or connective tissue showing a few bridges of trabecular bone tissue. A complete intervertebral arthrodesis was observed at this stage for all of the cases.

DISCUSSION & CONCLUSIONS: For all time periods considered, no local signs of intolerance was observed around the implant. The tested device allowed early fusion in the selected preclinical model. When actual fusion occurred within the implants, it was demonstrated that approximately 30 % of the implant volume degraded and resorbed. In spite of the low osteointegration of the device observed at early times, total implant material resorption and complete arthrodesis were obtained after 3 years of functional implantation in sheep. These results confirmed the capability of the implant to degrade without impairment of the device performance. Use of this resorbable spinal cage may be a valuable alternative to metals and non-degradable materials¹.

REFERENCES

¹D.S. Brodkle et al (2002) J Spinal Disord Tech 2002 **15**:206-212.

DOSE-EFFECT OF TRANSFORMING GROWTH FACTOR BETA3 ON DEGRADATION OF TRICALCIUM PHOSPHATE CERAMIC

B.Mahari¹, M.Glatt², T.Arvinte², M. Richter², E. Schneider¹, <u>B.A.Rahn</u> ¹

AO Research Institute, Davos Switzerland. ² Novartis Pharma, Basel, Switzerland.

INTRODUCTION: Transforming growth factor (TGF) beta3 is a polyfunctional regulatory cytokine out of the TGF beta superfamily. It has been shown to have roles in embryogenesis, soft tissue healing, tumor genesis as well as tumor suppression angiogenesis and osteogenesis. A clear effect of TGF-beta3 on cranial bone regenation has been observed in a preceding study in the rabbit using polylactic acid (PLA) as carrier.

Scaffoding matrices for bone repair should be of porous nature with interconnecting pores in dimensions similar to trabecular bone. Their components mimic mineralised bone and their degradation ideally goes hand in hand with replacement by newly formed bone. Even though many studies have been performed, the ideal material has not been found yet.

The purpose of this study was to determine an eventual dose related action of the growth factor on bone formation as well as carrier degradation.

METHODS: A paired cranial defect design was used in the rabbit. Dose effects of 10 µg/cm³, 50 μg/cm³ and 250 μg/cm³ were compared, using particulate Tricalcium phosphate (TCP) as a carrier. The observation time was 8 weeks. All animals received intravital labeling with bone seeking fluochromes in order to gain information on the timing of bone formation. The specimens were analysed using quantitative computed tomography, quantitative radiology and histomorphometry. For data analysis a "within animal" comparison was performed using a paired t-test for parametric data, and a Wilcoxon test for non-parametric data. "Between animals" comparisons were done in twosample t-tests for parametric data, and a Mann-Witney U-test for non-parametric data.

RESULTS: The evaluation of the radiographs as well as of the histological sections showed clear dose effects on the carrier: While the non-loaded control carriers within the same animals were not affected in all three dose groups, the tricalcium phosphate carrier loaded with the growth factor disappeared significantly faster with increasing dose. In the low dose group bone formation and carrier degradation were not significantly different to the non-loaded sites. Bone formation was

enhanced, but not significantly different between the two groups with a higher dose in spite of the fact that more space for the regenerate became available with increasing degradation.

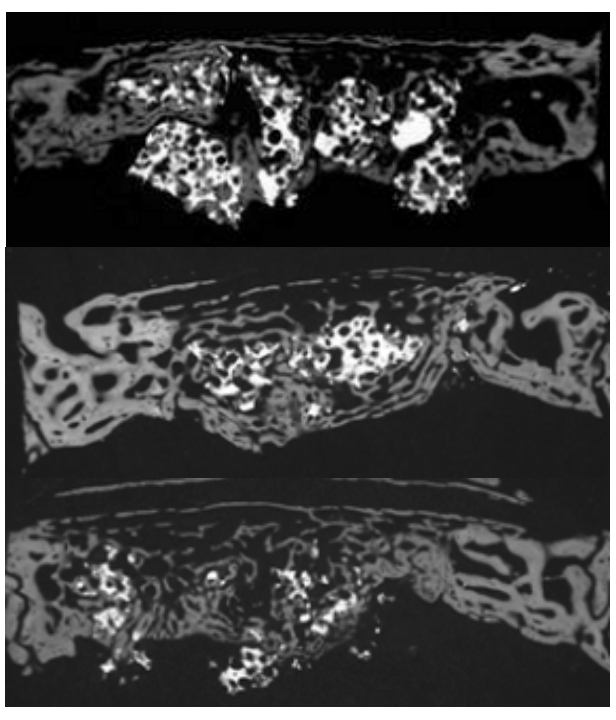


Fig. 1: Increasing influence of TGFbeta3 dose on the degradation of the ceramic carrier. Bony replacement of the carrier does not follow the speed of degradation. Top: low dose, middle: medium dose, bottom: high dose.

DISCUSSION & CONCLUSIONS: TGF-β3 has a significant, dose related effect on degradation of the TCP-carrier onto which it is loaded. A systemic action on carrier degradation at remote sites could not be shown. Additionally, this growth factor has a clear effect on bone regeneration. There are indications that there might be something like a therapeutic window near a dose of 50 μ g/cm³ in the early phase, and a direct dose / effect relationship at a later stage of bone regeneration. The exact mechanisms of dose dependence as well as the signaling pathway responsible for the time pattern of enhancement of bone regeneration remain unclear.

ACKNOWLEDGEMENTS: The authors thank R.Wieling, I.Keller and D.Pfluger for help in surgery, histology and statistics.

COPPER-ALUMINIUM BRONZE – A SUBSTITUTE MATERIAL FOR GOLD DENTAL ALLOYS?

P.Y. Eschler¹, H. Lüthy², L. Reclaru¹, A. Blatter¹, O. Loeffel², C. Süsz³, J. Boesch³. *PX Tech*¹, La Chaux-de-Fonds; University of Zurich²; Qualident³, Geneva; Switzerland

INTRODUCTION: Since the '80s, copperaluminium based alloys have appeared on the dental market in the US, Japan, South America and some countries of Eastern Europe. These aluminium bronzes, essentially a substitute for conventional gold-rich alloys, are employed for the fabrication of economical crowns and bridges¹. Alloyed with elements such as iron, nickel, manganese and tin, they show in fact quite a good colour match to gold, and they keep an astonishing brilliance in the oral environment.

Alloys used in dental restoration must have an appropriate corrosion resistance in order to avoid the release of cytotoxic or sensitising elements into the biological milieu. In this context, we have evaluated two commercial copper-aluminium dental alloys. We here present our results concerning their corrosion and tarnishing behaviour, as well as their release of nickel and copper ions.

MATERIALS AND METHODS: The test samples had the form of discs of diameter 11 mm. They were metallographically polished with diamond paste (granulometry 1 μm).

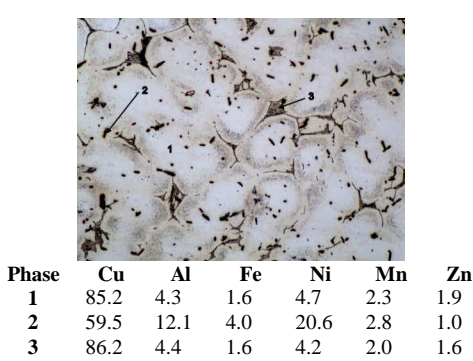


Fig. 1. Microstructure of alloy # A and phases composition (wt %).

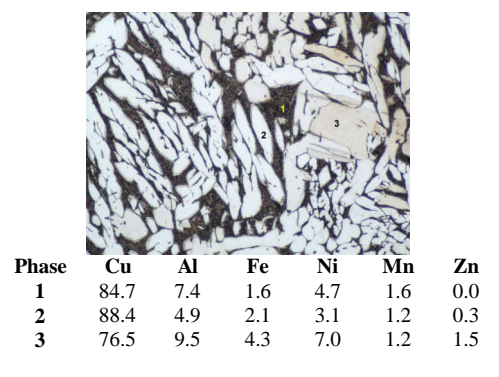


Fig. 2. Microstructure of alloy # B and phases composition (wt %.)

Table I. Composition of the tested aluminium bronzes (wt %).

Alloy	Cu	Al	Fe	Ni	Mn	Zn
# A	79.3	7.8	4.0	4.3	1.6	3.0
# B	82	10.7	2.5	3.55	1.2	0.05

Electrochemical measurements were conducted in artificial saliva of the Fusayama type (dearated with nitrogen, temperature 37° C, pH = 5) using the rotating electrode technique. The open-circuit potential (E_{oc}) was measured during 24 h. The polarization resistance (Rp) was calculated from the recorded linear polarization curves (Mansfeld curves). The cathodic and anodic potentiodynamic polarisation curves were measured from - 500 mV to + 1000 mV vs. SCE

A zonal coulometric analysis was derived from potentiodynamic polarization curves (zone I: from open-circuit potential (E_{oc}) up to + 300 mV; zone II: from + 300 mV to + 500 mV vs. SCE).

Tarnishing was evaluated in a thioacetamide test during two days. The test consists in exposure of the samples to the vapours emitted by thioacetamide in an atmosphere with a relative humidity of 75 %, maintained by the presence of a saturated solution of sodium acetate (ISO 4538).

Release tests were done by extraction in an 0.1 NaCl and 0.1 M lactic acid solution (temperature 37°C, рН 2.3, extraction = duration 7 days, sample surface to solution volume ratio: $1 \text{ cm}^2 / 1 \text{ ml}$). The copper and nickel ions released during into the solution during the test was quantitatively analysed by inductively coupled plasma spectroscopy (ICP).

RESULTS:

The potentiodynamic curves displayed in Fig. 3 reveal important differences in the behaviour of the aluminium bronze alloys (#A and #B) as compared to a conventional gold and a CoCr alloy.

The electrochemical parameters evaluated in deaerated artificial saliva are summarized in table II. All the results consistently show a much stronger corrosion susceptibility of the Cu-Al alloys as compared to conventional dental alloys.

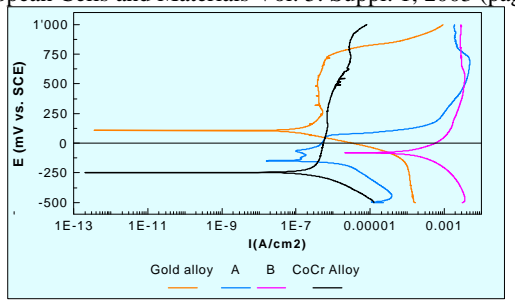


Fig. 3 Polarization curves of alloys # A and # B in comparison with a conventional gold and CoCr alloy.

Table II. Summary of the evaluated electrochemical parameters.

Alloy		5 0	Breakdown potential	Zonal coul	lometric analysis
	$\mathbf{E}_{\mathbf{oc}}$	$\mathbf{R}_{\mathbf{p}}$	$\mathbf{E_{bp}}$		+300 mV to + 500 mV
	[mV] vs. SCE	[kOhm/cm ²]	[mV] vs. SCE	[mC]	[mC]
A	- 144	6.1	97	839	3041
В	- 141	4.3	98	861	3505

During the electrochemical test, the surfaces of both alloys A and B have undergone a significant degradation as evidenced by SEM (Fig. 4). The apparent dendritic microstructure suggests a preferential dissolution of the interdendritic, copper-rich matrix.



Fig. 4. SEM micrograph of alloy # B after the potentiodynamic polarization measurement.

The release tests resulted indeed in high quantities of Cu and Ni in the electrolyte after 7 days (Fig. 5), accompanied by a sample total weight loss of 1.8 mg/cm² for alloy A and of 2.6 mg/cm² for alloy #B.

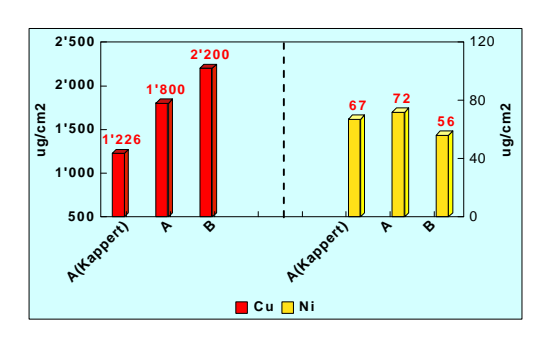


Fig. 5. Quantities of copper and nickel released after 7 days of immersion testing (included are independent results by Kappert²).

DISCUSSION AND CONCLUSIONS

According to our results, the two as-cast aluminium bronzes A and B exhibit a very low corrosion resistance in an oral-type environment. They release significant amounts of nickel and copper, and they tarnish much more than conventional gold alloys.

The release of cations like nickel may induce allergies. For the prevention of contact dermatitis, the European Directive 94/27/EC prohibits the commercialisation of products that come into prolonged contact with the skin, if they release more than 0.5 \(\text{ig/cm}^2\)/week of nickel. As seen in Fig. 5, the two aluminium bronzes release about 100 times this amount.

According to Kappert², the brilliance of these alloys is preserved in the mouth because of their uniform corrosion (i.e. they keep a polished look) and because the cytotoxicity of the released copper ions inhibits bacterial proliferation. On a microscopic level, however, we find a selective rather than an uniform corrosion.

From our results we conclude that this class of non-precious, aluminium bronze type III casting alloys present a very low corrosion resistance and an elevated release of problematic cations.

Reference

- 1. L. Reclaru, H. Lüthy, C. P. Marinello, P.Y. Eschler, C. Süsz, D. Bratu, Corrosion of Non-Precioua Type III Casting Alloys, *J Dent Res* 80: 712 (2001).
- 2. H. F. Kappert, M. Schuster, Dental Labor, XLIII, 3/2001

RETRIEVAL ANALYSIS OF SOME CEMENTLESS HA-COATED SMOOTH SURFACE ACETABULAR IMPLANTS

I Antoniac¹, D.Lãptoiu², M. Miculescu^{1*}, V.Bunea¹, F.Miculescu¹,

¹ Politehnica University from Bucharest, Romania, ² Colentina Clinical Hospital, Romania.

INTRODUCTION: The most common mechanism in total hip arthroplasties has been shown to be surface wear. Hydroxyapatite (HA) forms biological bonds between host bone and implant, being used as a surface coating for total hip arthroplasties since '80s [1]. Important questions still remain regarding the use of HA-coated acetabular components in total hip arthroplasty. Osteolysis due to bearing surface wear is the greatest unsolved problem that limits the durability of joint replacement. Retrieval studies of clinically well-functioning acetabular components should help to answer some of these questions.

METHOD: We examined four clinically successful HA coated cementless acetabular components retrieved at revision between 6 and 15 years after implantation. All components were of the same design (smooth-surfaced HA coated acetabular shell with two to three screws).



Fig. 1: Macroscopy view of the primary implant components who was analized: acetabular cup, poliethylene liner, screws.

The prostheses and the surrounding bone were qualitative histological prepared for and quantitative histomorphometric analysis [2]. The percentage of bone growth onto the implant, the relative bone area around the implant, the extent of residual HA coating, and the coating thickness were measured. Retrieved metallic shells were initially visually analyzed, then digital pictures were taken, areas of HA demarked and extent of bone ingrowth and HA absorption was analyzed. ESEM analysis was the next step, using two types of electron detectors: LFD and BED - composition images on shell surface and retrieved broken screws.

RESULTS: The primary implants - cementless HA coated smooth surface (Landos, France) had a HA coating of 60 micrometers thick and 5 screw holes on the surface. Tissues samples retrieved at the time of revision surgery for a migrated cementless acetabular implant associated with important osteolysis have consistent demonstrated histological pattern. All intraoperative bacteriological cultures were negative. The most common finding extensive was inflammation with a predominance of plasma cells and lymphocytes. Other anatomo-pathologic features included granulomas, foreign-body giant cells, necrosis, and fibrin exudation (figure 2). Each acetabular cup was removed with as much care as possible with regard of the bone stock and surrounding tissues. Gross inspection at the retrieved acetabular liners revealed a group of changes.

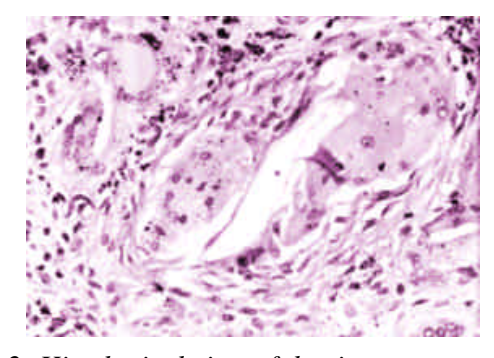


Fig. 2: Histological view of the tissue surrounding the implant under light microscopy. 1-foreign bodies, 2-foreign body inside giant cell, 3-giant cell and fibrin exudation; (hematoxilin Eosin, coloration of sample tissues; x 200)

Backside deformity with loss of machining lines, important backside markings around the screw holes, minimal wear inside the cup, advanced wear along the peripheral rim where impingement occurred. The digital analysis of the implants showed the degree of bone ingrowth at an average of 10 to 15% and the HA resorbtion extent averaged from 60 to 85% of the surface. ESEM analysis showed two patterns. The Ti6Al4V alloy type screws presents unhomogenous material, surface morphology analysis indicates a fatigue screw breakage type of failure, probably because of presence of the poliedric compounds with different composition compared with base metal (fig. 3).

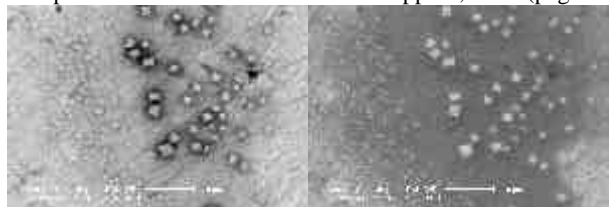


Fig. 3: Scanning Electron Microscopy (SEM) of the screw breakage area: left-BSE, right-LFD (x2931); note the poliedrical compounds with a visible different composition than surrounding metal basis, a possible source for weakness and failure.

The up surface of acetabular cup presents three different zones: base material porous type-titanium, remnant areas covered with hydroxy-apatite and areas polished by fretting (fig. 4).

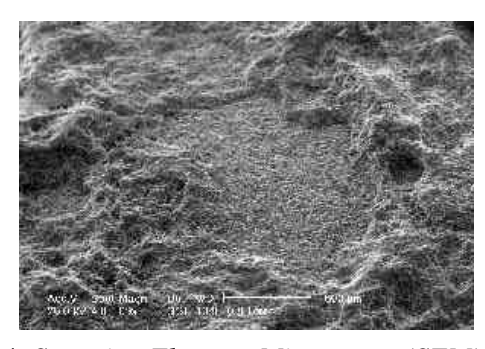


Fig. 4: Scanning Electron Microscopy (SEM) of the external surface of the acetabular shell (x69); note the difference in porosity between HA coated area and TiAlVa smooth metal surface.

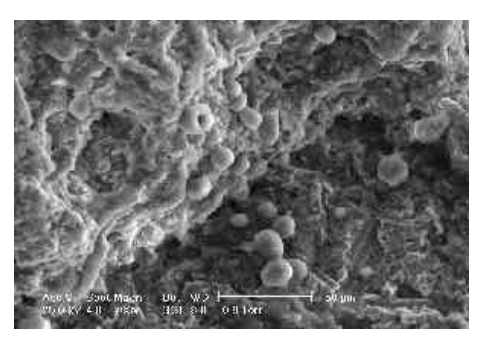


Fig. 5: Scanning Electron Microscopy (SEM) of the same area of the acetabular shell at the interface HA-metal (733X); note the important cell adhesions (bone and erythrocytes) related to the remnant HA in contrast with the smooth surface.

DISCUSSION & CONCLUSIONS: Regarding the fixation failure-poor biological fixation may be related to surgical errors at primary implantation; the best option is to have a porous surface HA-sprayed. Because of biocompatibility and osteoconductivity, HA coated implants, become stabilized by strong bone; whether macro or microtextured surface of the implant is better for bone-

ingrowth and prosthesis longevity is still a subject of debate [4]. The screws in acetabular fixation: usually not needed for press fit primary fixation they prevent rotation and tilt (good for revisions) but provide access for debris and development of "cold flow" mechanism. In our cases we think that the failure of the smooth surface HA coated implant occurred over time. It is not reasonable to expect soft tissue interlocking of such an implant, and with no osteointegration, the cup will be instable and fail. The screws not sufficiently well implanted at primary intervention became mobile and an initial source of debris. The screw holes reduced the potential area for bone ingrowth and became the entry for polyethylene debris in the acetabular bonetestimony being brought by the important screwhole markings on the backside of the polyethylene liner. The small particles are well known to produce a strong notch effect, in the gap created, oxygen content is consumed with a decrease in the local pH value of the body fluid and an increase of the corrosion rate. The added cell-mediated HA resorbtion seems to be the main reason for loss of HA coating. The area of bone ongrowth was within a certain range (15% to 40%) of the measured surfaces, and it was independent of the amount of HA residue. The excessive wear generated important debris and the inflammatory answers of the organism lead to osteolysis, excessive HA restoration and failure of the acetabular cup. The analyzed failure cases may be caused by the inaccurate insertion of the cup with inefficient screws that led to a combination of metal and polyethylene debris disease. After an initially normal clinical evolution, the local biological and mechanical factors led to failure of the initially good but insufficient lamellar bone and eventually bony bridges.

REFERENCES: ¹ RJ. Furlong, JF Osborn (1991) Fixation of hip prosthesis by hydroxiapatite ceramic coatings *in J.Bone Joint Surgery 73:741-745* ² P. Frayssinet, D. Hardy, P. Conte, P. Delince, A. Guilhem, G. Bonel (1993) Histological analysis of the bone-prosthesis interface after implantation in humans of prostheses coated with hydroxyapatite *in J Orthop Surg 7:246-253*, ³ D. Bunea, V.Antoniac et al. (1999) *Implant Materials, Printech Ed., 1999, pp. 80-85* ⁴ P. Laffargue, JA Helsen, HJ Breme, HF Hildebrand (1998), Retrieval analysis *in Metals as Biomaterials, J.Wiley & Sons Ltd, pp. 469-472*.

EXPERIMENTAL RESEARCHES CONCERNING THE Co-Cr-Mo ALLOYS USED IN IMPLANTOLOGY

D.Bunea*, D.Bojin, S.Zamfir, F.Miculescu, M.Miculescu

Politehnica University from Bucharest, Romania

INTRODUCTION: Co-Cr-Mo alloys are used on a large scale in implants and prosthetics. The researches that are presented in this article, highlight the study of corrosion behavior and testing in environments of cellular cultures of an F75 ASTM alloy, used on a large scale in the entire world at the performing of implants and prosthesis. The aim of the researches consisted in obtaining the necessary results for establishing the implantation duration of the products performed from this biomaterial, elaborated in "Politehnica" University of Bucharest laboratories.

The researches were performed on Co-Cr-Mo alloy type, with the chemical composition specified according to ASTM F75. The main characteristic of this alloy is represented by its corrosion resistance in chloride environments, which is owed to both chemical composition and oxide formed on its surface (Cr_2O_3) .

METHODS: To achieve the proposed objective there have been carried out tests concerning the cellular viability tests, corrosion tests, in two environments that stimulate the existent conditions in the human organism and also scanning electron microscopy investigation and EDS spectrometry over the samples subjected to the above mentioned tests. The alloy elaboration has been performed in a kiln in vacuum of Baltzers type heated at 1350/1450⁰ C and cast in bar shaped ceramic mould of 20mm diameter of cocsofemural tail prosthesis. The metallographic samples taken from the casting profile have been submitted to some initial investigations by a XL 30 ESEM scanning electron microscope, made by Phillips.

To confirm one of these aspects that express the biocompatibility of the analyzed alloy, the sample has been subjected to cellular viability tests, by increasing some fibroblast cellular cultures in the presence of the sample.

After performing these cellular viability tests, the sample has been prepared for corrosion tests in vitro, by cleaning in acetone and deionizer water with ultrasounds for 60 minutes.

The corrosion samples behavior was studied in two environments: artificial saliva and artificial

physiologic solutions. The samples were immersed for 8 hours in the above mentioned solutions, and the tests were performed in special recipient protected against ventilation. It was determined the value of electrode potential of each sample in each solution and the modification of this potential has been recorded automatically from 5 to 5 minutes.

order to establish the morphological modifications that appeared on the sample surface after performing the corrosion tests, the samples were analyzed by scanning electron microscopy, being obtained some images of the surface morphology [1,2]. (Secondary electrons images SE), images showing the compositional differences that appeared on the surface of the analyzed sample (backscattered electrons images BSE), and also morphological micrographs, by mixing secondary electrons signal with the backscattered electrons signal (Mix images).

Over the surfaces there have been performed EDAX quantitative compositional analyses and also analyses concerning the elemental distribution on corroded zones (mapping).

RESULTS: The determination of the chemical composition of the obtained alloy was made on samples obtained from the processed bar. The compositional analyzes was obtained with a spectrometer after an energy of EDAX type.

Table 1 EDAX compositional analyzes of Co-Cr-Mo alloy.

Element	Wt %	At %
AlK	0.22	0.47
SiK	1.01	2.06
MoL	5.57	3.32
CrK	27.70	30.49
MnK	0.35	0.36
FeK	0.60	0.62
CoK	63.54	61.70
NiK	1.01	0.98
Total	100.000	100.000

The results of the quantitative chemical composition analyses showed in table 1, confirms the alloy situation in F75 class, according to ASTM.

European Cells and Materials Vol. 5. Suppl. 1, 2003 (pages 53-54) The study of the behavior in cellular culture environment of the selected alloy was established in comparison with the test performed on a pure titanium sample, by apoptosis analyzing.



Fig. 1: Optical microscopy image in phase contrast for the Co-Cr-Mo sample at 20x magnification (left), and optical microscopy image in phase contrast for the etalon titanium sample, at 20x magnification (right).

With the displayed data obtained after the corrosion test, it was elaborated the electrode potential variation curve. (Figure 2)

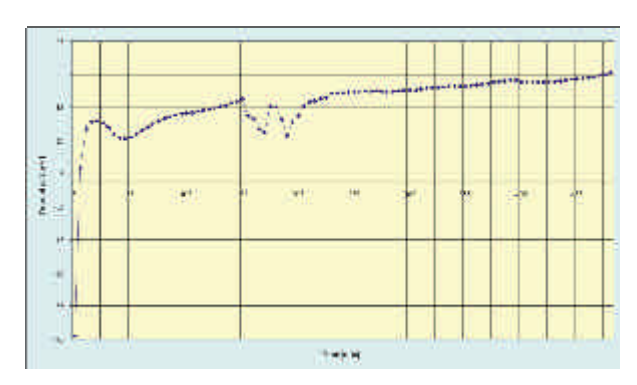


Fig. 2: Electrode potential variation curve for the test performed in artificial saliva environment.

In figures 3 and 4 are presented two micrographs where the surface morphology is tested in artificial saliva environment, thoroughly the surface morphology immersed in artificial physiologic solution.

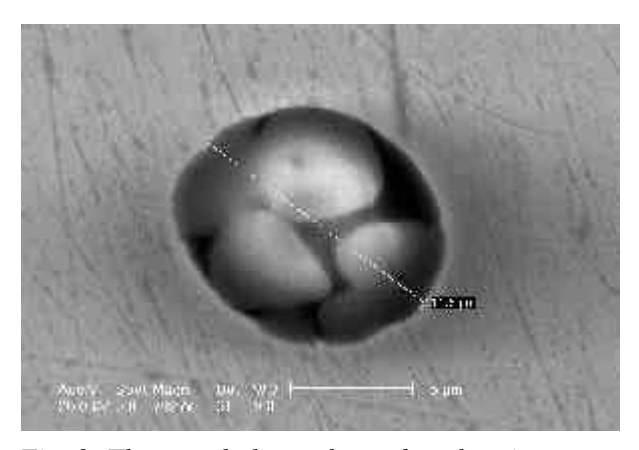


Fig. 3: The morphology of tested surface in artificial saliva environment.

DISCUSSIONS & **CONCLUSIONS**: F75 ASTM, Co-Cr-Mo alloy, presents important characteristics from the biocompatibility point of view, what recommends it for the usage at the obtaining of implants and prosthesis. The results of corrosion tests processed by our reserches highlights the fact that the alloy is pitting corroded due to submicron defects that appeared beyond casting and solidification [2,3].

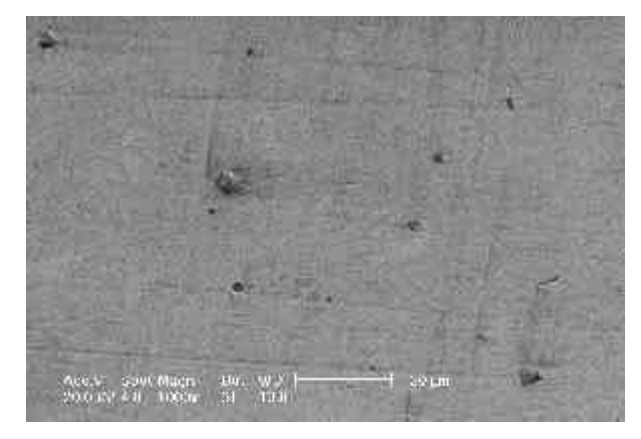


Fig. 4: The morphology of the surface immersed in artificial physiological solution.

Due to very good characteristics of corrosion resistance, the biomaterial is auto-passivated, resisting very well to the attack of corrosive factors from the human organism, so this alloy is recommendable for processing implants and prosthesis with a long term usage.

REFERENCES: ¹ Joseph D. Bronzino (1995) *The Biomedical Engineering Handbook*, Hartford Conecticut, 537-552; ² Merritt, K. and Brown, S.A. (1996) *Distribution of cobalt-chromium wear and corrosion products and biologic reactions*, Clin. Orthop. Rel. Res. 329, 233-43; ³ Shahgaldi BF, Heatly FW. Dewar A, Corrin B. (1995) *In vivo corrosion of cobalt –chromium and titanium wear particles*, J. Bone Joint Surg Br., 77(6); 962-966.

OSTEOBLASTS RESPONSE TO BONE SUBSTITUTES IN VITRO

Omana A. Trentz¹, Simon P. Hoerstrup³, Li K. Sun¹, Lukas Bestmann⁴, Andreas Platz², Otmar L.Trentz²,

Research Division (PD G. Zund)¹, Division of Trauma Surgery (Prof. O. Trentz)², Division of Cardio-vascular Surgery (Prof. M. Turina)³, Department of Surgery and Institute for Clinical Chemistry (Prof. A. von Eckardstein)⁴, University Hospital Zurich, Switzerland

INTRODUCTION:

The repair of large osseous defects still represents an unsolved problem in bone surgery. The use of autogenous bone grafts is widely accepted and considered to be the "golden standard" in the bone defects. However, treatment of disadvantages of autogenous bone grafts are limited availability, harvesting morbidity, and insufficient biomechanical properties. problems with autografts have initiated the development of several allogenic, xenogenic, and synthetic bone graft alternatives. complication rate due to interaction between biomaterials and host tissues could be reduced. Still cell-mediated immune responses, as well as synthesis and resorption processes by osteoblasts and osteoclasts respectively are not yet fully controllable. The main problem in clinical use remains osteoclastic resorption and remodelling, representing a crucial issue of long term mechanical stability. Furthermore, vascularisation involvement of neuronal fibres neuropeptides are very important for development, growth, and differentiation of bone cells and matrix.

The present investigation has focused on the biocompatibility of allogenic and xenogenic solvent dehydrated cancellous bone (SDCB) with phenotypic osteoblasts *in vitro*.

MATERIAL AND METHODS:

Allogenic and Xenogenic Solvent Dehydrated Cancellous Bone (SDCB) from human and bovine femoral necks were prepared, 14 mm diameter and 3 mm thickness to fit into the 24 well plates, for our experiment *in vitro*.

Human osteoblasts were harvested from the cancellous bone (iliac crest), obtained under sterile conditions from patients undergoing ORIF with bone grafting. Specificity of the primary human osteoblast was controlled by biochemical marker of osteoblasts alkaline phosphatase (ALP) and Osteocalcin (OC). All patients provided informed consent.

Cell proliferation: Cytotoxicity and cell proliferation were determined by the **MTT-Test**.

The MTT [3-(4,5 dimethyl-thiazol-2-yl)2,5-diphenyltetrazolium bromide]- based on colorimetric assay as described by Mosmann.

Osteocalcin: OC was measured by a non-radioactive ELISA kit (Dako, Switzerland) in conditioned medium, which was collected on day 1, 3, and 7 and frozen at minus 80°C.

Reverse Transcription Polymerase Chain Reaction (RT-PCR):

RNA for Osteocalcin (OC) and Alkaline Phosphatase (ALP) was extracted from confluent primary human osteoblasts cultured on human and bovine SDCB and as control the cells without SDCB discs with an Qiagen RNase Kit (Hilden, Germany). As control we used the housekeeping gene glyceraldyde-3-phosphate dehydrogenase (GAPDH). The amplification primer sets for PCR were from the NCBI nucleotide database.

Cell Morphology: For SEM cells seeded discs were fixed with 2.5% glutaraldehyde (pH 7. 3) on day 7, 14, and 21.

RESULTS: There was no significant difference by the MTT-Test between the human and bovine discs compared to control without discs. Osteocalcin level was significantly lower with human discs on day 3, and increased on day 7. In RT-PCR, **ALP** and **OC** gene expression did not show difference compared to control. SEM showed completely homogenous distribution of the cells and were growing into the pores to integrate throughout the scaffold.

CONCLUSION:

In conclusion, our *in vitro* observations suggest that SDCB may be a suitable bone substitute which provides a well structured and biocompatible scaffold for ingrowing human osteoblasts.

THE INFLUENCE OF FLUORIDE IONS ON THE CORROSION RESISTANCE OF TITANIUM AND NITI IN AN ARTIFICIAL SALIVA AND A MOUTHWASH

N.Schiff¹, B.Grosgogeat¹, M.Lissac¹, F.Dalard²

¹ School of dentistry, Lyon, France.
² LEPMI, polytechnic institut of Grenoble, Saint Martin d'Hères, France

INTRODUCTION: Nowadays, in oral implantology, Titanium is the best material. In dental orthopedic procedures, Nickel-Titanium alloys are frequently used. At the same time, fluoride mouthwashes are more and more prescribed by practitioners.

The aim of this work is to study the corrosion resistance of pure Titanium and NiTi alloy, in a reference medium and a mouthwash.

METHODS: The materials chosen are already prepared for clinical used, implantology for Titanium and orthodontic treatments for NiTi. The samples were shaped into a cylindrical form, in order to constitute the cap of rotating disk electrode. They were mechanically cleaned with abrasive strips and tested in three media: Fusayama Meyer artificial saliva ¹, fluorided and acidified Fusayama Meyer artificial saliva and Acorea® ready to use mouthwash.

The electrochemical setting employed is a glass electrochemical cell with a calomel saturated electrode, a platinium cunter electrode and a working rotating disk electrode in a Faraday cage, all connected to a potentiostat with a specific software, obtaining potentiometric and polarization curves.

The corrosion resistance is studied by getting different values: corrosion potential, density of corrosion current and polarization resistance.

Afterwards, by a chronoamperometric study we get samples to be analyzed at the S.E.M.

RESULTS: The values obtained show a clear decreasing of the corrosion resistance of the two tested materials when used in the acidified and fluorided environment. In the Acorea® mouthwash we also observed a decrease in electrochemical properties of these two materials and the S.E.M. shows a deterioration of the surface of specimens² (table 1).

Table 1. Corrosion potentials and polarization resistance of NiTi alloy.

NiTi	Fusayama Meyer Artificial saliva	Acorea ^R Mouthwash
Corrosion potential	-150 mV/SCE	-380 mV/SCE
Polarization Resistance	120 KÙ.cm²	40 KÙ.cm²

DISCUSSION & CONCLUSIONS: It is clearly experimented that the corrosion resistance of the two specimens decreases in the presence of fluoride in an acid environment ^{3, 4}. Fluoride dissolve the protective oxide layer of the materials. In artificial saliva, a chemical attack is visible at SEM, characterized by localized pitting. The Acorea® mouthwash, with a pH=5 and a fluoride concentration of 65ppm, has the same effect that fluorided and acidified artificial saliva but is less aggressive. The two materials have also a deterioration of the passive layer, visible at S.E.M. as generalized corrosion.

So, it seems wiser not to use certain fluorided mouthwashes especially during long terms orthodontic procedures, to avoid the risk of loosing physical and electrochemical characteristics of used materials. Moreover, in the presence of fluoride ions, there could be nickel ions release which are known to cause toxic and allergic reactions in the body.

REFERENCES: ¹ VW. Leung (1997) Artificial salivas for in vitro studies of dental materials, J Dent 25:475-84. ² MH. Kononen and all (1995) observations on stress corrosion cracking of commercially pure titanium in a topical fluoride solution, Dent Mater 11:269-72. ³ G. Boere (1995) Influence of fluoride on titanium in a acidic environment measured by polarization resistance technique, J Appl Biomater 6:283-88. ⁴ L. Reclaru, JM. Meyer (1998) Effects of fluorides on titanium and other dental alloys in dentistry, Biomaterials 19:85-92.

ACKNOWLEDGEMENTS: thanks to Ormodent and Timet Savoie for providing the different materials.

CELL BEHAVIOUR OF RAT CALVARIA BONE CELLS ON NITI WITH DIFFERENT SURFACE ROUGHNESSES

C.Wirth¹, C.Lagneau¹, P.Exbrayat¹, L.Ponsonnet², M.Lissac¹

INTRODUCTION: Nickel-titanium alloys (NiTi) are metallic biomaterials known for their superelastic and shape memory properties [1]. These properties suggest that it could be used for medical purposes such as surgical implants. The interactions between cells and implants are influenced by a number of physical and chemical processes, among which, a major factor is the implant surface roughness [2,3]. The purpose of this study was to examine the behaviour of rat bone cells cultured *in vitro* on NiTi with different surface roughnesses.

METHODS: NiTi plates were mechanically polished with wetted metallographic polishing (grade 400 and 2400) SiC papers. According to the paper grade used, the samples will be referred to NiTi 400 and NiTi 2400. To determine the surface topography, prepared NiTi disks were observed with scanning electron microscopy (SEM) and examined for average surface roughness (Ra) with a profilometer. The cells were obtained after collagenase digestion of neonatal rat calvaria as described by Nefussi et al. (1985). The cell morphology, the proliferation and the synthesis of extracellular matrix protein (type I collagen and fibronectine) was studied. The morphology of the cells was analysed after 120 min and 15 days of culture with a Hitachi S800 scanning electron microscope. The proliferative activity of cultured cells was determined with the MTT colorimetric assay as described by Mossman (1983), at 2, 4 and 7 days seeding. After 7 days, cultured bone cells were prepared for immunofluorescence staining.

RESULTS: The average value of roughness profile (Ra) was equal to 0.07 μm for NiTi 2400 and 0.15 μm for NiTi 400. The SEM micrographs (Figure 1) showed the difference in density size of the grooves between these two sustrates. Figure 2 showed cellular morphology after 120 min of culture on NiTi. The cells adhered to their support by thin cytoplasmic digitations or filopodia. After 15 days of culture, cells had multilayered and organized in nodules of various sizes and shapes. No particular orientation of the cells was observed for all the samples. The MTT assay releaved that

cells cultured on NiTi 400 showed high rates of proliferation. After 7 days, an intracellular labeling was obtained with anti-fibronectin and type I collagen antibodies. Fluorescence was intense around the nucleus and more diffuse in the rest of the cytoplasm.

Fig. 1: SEM images of NiTi 2400 (left) and NiTi 400 (right).

Fig. 2: SEM images of osteoblastic cells cultured on NiTi 2400 (left) and NiTi 400 (right) at 120 min after seeding.

DISCUSSION & CONCLUSIONS: Rat'embryo osteoblastic cells were shown to respond specifically to two closely related biomaterials, NiTi 400 and NiTi 2400. The cell proliferation was significantly greater on NiTi 400 than on NiTi 2400. No significant difference between the synthesis of extracellular matrix protein (collagen and fibronectin) was obvious through immunofluorescence staining.

REFERENCES: ¹ L. Jourdan, MP. Filleul, R. Portier (1997) *Rev Orthop Dento Faciale* **31**:199-211. ² B. Chehroudi, TR. Gould, DM. Brunette (1991) *J Biomed Mater Res* **25**:387-405. ³ K. Hatano, H. Inoue, T. Kojo, T. Matsunaga, T. Tsujisawa, C. Uchiyama, Y. Uchida (1999) *Bone* **25**:439-445.

¹ Laboratoire d'étude des interfaces et des biofilms en odontologie – Faculté d'odontologie de Lyon, FRANCE.

² Laboratoire d'ingénierie et fonctionnalisation des surfaces – Ecole centrale de Lyon, FRANCE.

BIODEGRADABLE POLYMERS FOR BIOMEDICAL APPLICATIONS

Etienne Schacht

Polymer Materials Research Group, UGent, Krijgslaan, 281, B-9000 Ghent, Belgium etienne.schacht@rug.ac.be

INTRODUCTION: Polymers are applied for a large number of medical applications: as medical supplies, as support or replacement of malfunctioning body parts or as a drug reservoir providing a local therapeutic effect. The specifications for the selected material strongly depend on the application. For temporary applications, biodegradable polymers may be the preferred candidate. In the past 3 decades, a large range of biodegradable polymers have been developed, tested and applied for a wide variety of medical applications. A recent development in biomaterial science is the use of polymers as scaffolds for tissue engineering and regenerative medicine. Biodegradable polymers are the preferred candidates for making such constructs. In addition there is the growing need to provide biodegradable polymers which also interact in a favourable way with the external biological environment as to stimulate cell ingrowth and tissue regeneration. This can be achieved by loading the scaffold with bioactive molecules or by surface modification of the scaffold.

BIODEGRADABLE HYDROGELS

Hydrogels are interesting materials for medical application, including drug delivery systems and matrices for cell culture. As part of our biomaterials project we have developed biodegradable hydrogels either based on biopolymers or on poly(ethylene glycol) (PEG). In the first case the biopolymer, gelatine and/or agarose, was chemically modified in order to introduce groups polymerisable side (methacrylamide, methacrylate). Aqueous solutions of biopolymers can "solidify" by physical structuring and then be chemically crosslinked. The ratio crosslinkage/chemical crosslinkage can be controlled. Moreover, by means of simple cryogenic treatment phase separations can be achieved which lead to porous materials.

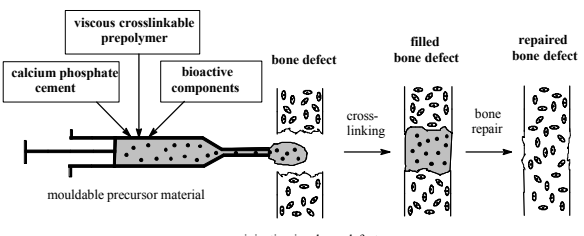
Biopolymer based hydrogels have been evaluated as materials for wound treatment. As an alternative, bismacromers of PEG containing well defined biodegradable segments were prepared and consequently crosslinked. The degradable segment is a depsipeptide consisting of one amino acid and either lactide or glycolide. By varying the depsipeptide composition, the rate of degradation of the hydrogel can be controlled. Such materials can be fine-tuned for a given application.

IN SITU CROSSLINKABLE BIODEGRADABLE POLYESTERS AND POLYORTHOESTERS

Starting from lactide, glycolide and/or caprolacton, and a diol as initiator, prepolymers with terminal HO-groups can be prepared. The latter can be easily converted into crosslinkable methacrylates.

By proper choice of the comonomers and the molecular weight of the prepolymer, viscous materials can be prepared which allow mixing with additives, such as porogens, calcium phosphates and biomolecules. Such mixtures can be applied into a bone cavity and then crosslinked, e.g. photochemically. The porogen is a water soluble particle which leaches out and creates pores of a given size. Such materials can be used for treatment of bone defects as well as for the fixation of metal implants, e.g. dental implants.

More details about the synthesis and properties of these biodegradable polymers and their biomedical application will be discussed in the presentation.



injection in a bone defect